https://doi.org/10.1038/s41591-023-02363-y

# Anti-GD2 CAR-NKT cells in relapsed or refractory neuroblastoma: updated phase 1 trial interim results

Received: 23 August 2022

Accepted: 24 April 2023

Published online: 15 May 2023

Andras Heczey[1,2] ✉, Xin Xu[1], Amy N. Courtney[1], Gengwen Tian[1], Gabriel A. Barragan[1], Linjie Guo[1], Claudia Martinez Amador[1], Nisha Ghatwai[1], Purva Rathi[1], Michael S. Wood[1], Yanchuan Li[1], Chunchao Zhang[1], Thorsten Demberg[1], Erica J. Di Pierro[1], Andrew C. Sher[3], Huimin Zhang[2], Birju Mehta[2], Sachin G. Thakkar[2], Bambi Grilley[2], Tao Wang[4], Brian D. Weiss[5], Antonino Montalbano[6], Meena Subramaniam[6], Chenling Xu[6], Chirag Sachar[6], Daniel K. Wells[6], Gianpietro Dotti[7] & Leonid S. Metelitsa[1,2] ✉

Vα24-invariant natural killer T cells (NKTs) have anti-tumor properties that can be enhanced by chimeric antigen receptors (CARs). Here we report updated interim results from the first-in-human phase 1 evaluation of autologous NKTs co-expressing a GD2-specific CAR with interleukin 15 (IL15) (GD2-CAR.15) in 12 children with neuroblastoma (NB). The primary objectives were safety and determination of maximum tolerated dose (MTD). The anti-tumor activity of GD2-CAR.15 NKTs was assessed as a secondary objective. Immune response evaluation was an additional objective. No dose-limiting toxicities occurred; one patient experienced grade 2 cytokine release syndrome that was resolved by tocilizumab. The MTD was not reached. The objective response rate was 25% (3/12), including two partial responses and one complete response. The frequency of $CD62L^{+}$NKTs in products correlated with CAR-NKT expansion in patients and was higher in responders ($n = 5$; objective response or stable disease with reduction in tumor burden) than non-responders ($n = 7$). *BTG1* (BTG anti-proliferation factor 1) expression was upregulated in peripheral GD2-CAR.15 NKTs and is a key driver of hyporesponsiveness in exhausted NKT and T cells. GD2-CAR.15 NKTs with *BTG1* knockdown eliminated metastatic NB in a mouse model. We conclude that GD2-CAR.15 NKTs are safe and can mediate objective responses in patients with NB. Additionally, their anti-tumor activity may be enhanced by targeting BTG1. ClinicalTrials.gov registration: NCT03294954.

Despite the remarkable progress achieved using chimeric antigen receptor (CAR)-T cells to treat hematologic malignancies, patients with solid cancers remain largely resistant to this type of immunotherapy[1]. Factors that contribute to this resistance include heterogeneous infusion products containing cells with variable anti-tumor potential, poor trafficking of conventional T cells to tumor sites, inhibition of T cell effector functions in the tumor microenvironment and tumor escape via antigen loss or other mechanisms[1]. Pharmacological and

A full list of affiliations appears at the end of the paper. ✉e-mail: heczey@bcm.edu; lsmeteli@txch.org

**Table 1 | Patient characteristics**

| | N | Age, years | Gender | Ind | Cons | Maint | S1 | S2 | S3 | S4 | S5 | INSS | Involved sites | SC | N-Myc status |
|---|---|---|---|---|---|---|---|---|---|---|---|---|---|---|---|
| Dose level 1** | 1 | 12 | M | A | C1 | M* | S1 | B | | | | 4 | Multifocal bone and bone marrow, soft tissues and paraspinal masses | UF | A |
| | 2 | 12 | M | A | C2 | M | S2 | B | S8 | S2 | | 4 | Multifocal bone | UF | NA |
| | 3 | 6 | M | A[#] | > | > | S2 | B+X | M | S2 | | 4 | Multifocal bone | UF | NA |
| Dose level 2 | 4 | 11 | F | A | C1 | M | R | S6 | B+V | S4 | | 4 | Multifocal bone | UF | UK |
| | 5 | 7 | F | A+B | C1 | > | S2 | B+D | S | S+T | | 4 | Multifocal bone, bone marrow and soft tissue | UF | NA |
| | 6 | 6 | F | A+B | C3 | M | S3 | S2 | | | | 4 | Multifocal bone, bone marrow and soft tissue | UK | A |
| Dose level 3 | 7 | 7 | F | A | C1 | M* | B | X | | | | 4 | Multifocal bone | UF | NA |
| | 8 | 4 | M | A+B | C3 | M | S2 | | | | | 4 | Multifocal bone, bone marrow | UF | NA |
| | 9 | 2 | F | A | C3 | M% | S4 | S7 | | | | 4 | Multifocal bone, large soft tissue mass | UF | A |
| Dose level 4 | 10 | 9 | M | A | C3 | M | S2 | | | | | 4 | Soft tissue and bone | UF | NA |
| | 11 | 12 | M | A | C2 | M | S5 | S2 | S9 | S2 | | 4 | Bone and bone marrow | F | NA |
| | 12 | 5 | M | A[#] | > | > | S2+R | [&]+C3 | M | DFMO+E | S2 | 4 | Multifocal bone | UF | NA |

**Patients previously reported[28]. Ind, induction; A, five-cycle induction with resection; B, high-dose MIBG therapy (HD-MIBG) with stem cell rescue (SCR). [#]Did not complete induction due to suboptimal response. Cons, consolidation; C1, carboplatin, etoposide, melphalan + SCR, radiation therapy (XRT); C2, busulfan, melphalan (BuMel) + SCR, XRT; C3, Thiotepa/Carbo + SCR; BuMel + SCR, XRT. Maint, maintenance; M, dinutuximab + *cis*-retinoic acid. *Difluoromethylornithine (DFMO) after completion on maintenance. [%]Stopped after three cycles due to progression. S, salvage; S1, irinotecan/temozolomide; S2, dinutuximab/GM-CSF/irinotecan/temozolomide; S3, tremetinib; S4, topotecan/cyclophosphamide; S5, irinotecan/temozolomide/alisertinib; S6, vincristine/irinotecan/temozolomide; S7, irinotecan/temozolomide/lorlatinib; S8, HDM201; S9, cyclophosphamide and zoledronic acid; R, resection; B, HD-MIBG; X, XRT; D, dinutuximab. [&]Cycle 5 of induction; V, vorinostat; S, selumetinib; T, temsirolimus; E, etoposide; INSS: International Neuroblastoma Staging System; SC, Shimada classification; F, favorable; UF, unfavorable; A, amplified; NA, non-amplified; UK, unknown status.

genetic engineering approaches are being employed to overcome the inherent limitations of bulk T cells for CAR-redirected immunotherapy[2,3]. In parallel, other types of immune effector cells with innate anti-tumor properties, such as natural killer (NK), natural killer T (NKT) and gamma/delta T cells, are being actively explored as alternative carriers for CARs or other tumor-specific receptors[4–7].

Neuroblastoma (NB) is one of the most common and deadly solid tumors of childhood[8]. Forty-five percent of patients have high-risk disease at diagnosis, of whom only approximately 50% remain in remission long term despite the availability of multi-modal treatments, including intensive myeloablative chemotherapy, stem cell transplantation, retinoic acid therapy and anti-GD2 antibody dinutuximab[9]. The GD2 disialoganglioside, which is selectively expressed at high levels in most NB tumors, has become a target for development of cellular immunotherapy using GD2-specific CARs[10]. Early phase 1 clinical trials evaluating GD2-CAR-T cells showed that the therapy was safe but generated few durable clinical responses[11–14]. This created an opportunity for employing alternative cellular platforms in the development of novel NB immunotherapeutics that target GD2 and other clinically validated tumor-associated antigens.

Vα24-invariant NKTs are a sublineage of innate-like T cells that express the Vα24-Jα18 invariant T cell receptor (TCR) α-chain and react to glycolipids presented by CD1d, in particular α-galactosylceramide (αGalCer)[15]. Unlike conventional T cells, NKTs constitutively express receptors for chemokines produced by NB cells and demonstrate effective trafficking to tumor sites in a xenogeneic NB model[5]. NKTs are also characterized by a suite of natural anti-tumor properties, including the ability to directly kill tumor cells expressing CD1d (ref. 16), targeting tumor-associated macrophages[17,18] and activating anti-tumor NK and T cell responses[16,19]. In patients, the presence of NKTs in primary tumor tissues[20,21] and NKT frequency in the peripheral blood[22] have been associated with positive clinical outcomes in several types of cancer. Together, these findings justify the development of NKT-based cancer immunotherapies.

To overcome the challenge of low endogenous NKT frequency, several groups developed methods to enrich for and expand NKTs ex vivo before adoptively transferring the cells into patients with cancer[23,24]. NKT products that were generated using these methods and used to treat patients on multiple clinical trials were associated with excellent safety profiles and mediated some clinical responses. However, these cell products had either low (below 10%) or variable (10–90%) purity, making it difficult to accurately interpret results[23,25–27]. We developed a Good Manufacturing Practices (GMP)-compatible protocol to isolate and expand clinically relevant numbers of NKT cells, allowing us to manufacture consistently pure NKT products that can be engineered to express therapeutic transgenes[5]. In the first clinical application of this technology, we initiated a phase 1 trial evaluating autologous NKTs expressing a GD2-specific CAR and interleukin 15 (IL15) (GD2-CAR.15) in children with relapsed or resistant NB. Interim results from three patients on dose level (DL) 1 demonstrated the safety of CAR-NKTs in patients with NB and the feasibility of our GMP protocol[28]. We found that CAR-NKTs expand in the peripheral blood after infusion, traffic to metastatic sites and induce tumor regression in heavily pre-treated, relapsed/refractory patients[28]. We have now completed enrollment and assessment of 12 patients on this study treated on four DLs, providing additional data points to assess CAR-NKT safety, anti-tumor activity and immunological correlates in relationship to the given or achieved dose.

## Results

### Trial design and safety data

The primary objective was to define the safety profile of autologous GD2-CAR NKTs and determine the maximum tolerated dose (MTD). We infused 12 patients (median 7 years of age, range 2–12 years, female 5/12) with stage 4 relapsed or refractory high-risk NB between 20 August 2018 and 17 December 2021 (Table 1 and Extended Data Fig. 1). Interim results from patients 1, 2 and 3 were previously reported[28]. Of 31 patients assessed for eligibility, 17 were excluded and 14 were

**Table 2 | Safety characteristics of GD2-CAR.15 NKT cell treatments**

| Body system | Event | Grade | |
|---|---|---|---|
| | | 3 | 4 |
| Blood and lymphatic system disorders | Anemia | 5 | |
| | Leukopenia | 5 | 6 |
| | Lymphopenia | 1 | 9 |
| | Neutropenia | 1 | 11 |
| | Thrombocytopenia | 1 | 3 |
| Gastrointestinal disorders | Abdominal distension | 1 | |
| | Acute gastroenteritis | 1 | |
| | GGT increase | 1 | |
| | Vomiting | 1 | |
| General disorders conditions | Fatigue | 1 | |
| Metabolism and nutrition | Hyperkalemia | 3 | |
| | Hypokalemia | | 1 |
| | Hypophosphatemia | 1 | |
| Musculoskeletal and connective tissue disorders | Bone pain | 1 | |
| | Headache | 1 | |
| | Neck pain | 1 | |
| Infectious disorders | Fever and neutropenia | 1 | |
| | Urinary tract infection | 1 | |
| Nervous system disorders | Altered mental status | 1 | |
| Respiratory, thoracic and mediastinal disorders | Hypoxia | 1 | |
| Miscellaneous | Proteinuria | 1 | |

AEs were collected from the beginning of lymphodepletion (day −4) until day 28 after infusion and graded according to the Common Terminology Criteria for Adverse Events version 4.

**Table 3 | Anti-tumor activity of GD2-CAR.15 NKTs in patients**

| | N | Curie score | | Response per INRC | |
|---|---|---|---|---|---|
| | | Pre-infusion | Post-infusion | After 1st infusion | After 2nd infusion |
| Dose level 1 | 1 | 21 | 21 | SD | |
| | 2 | 2 | 1 | PR | PR |
| | 3 | 7 | 5 | SD | |
| Dose level 2 | 4 | 15 | 17 | PD | |
| | 5 | 25 | NM | PD | |
| | 6 | 19 | NM | PD | |
| Dose level 3 | 7 | 5 | 5 | SD | |
| | 8 | 10 | 21 | PD | |
| | 9 | 3 | NM | PD | |
| Dose level 4 | 10 | 3 | 0 | PR | CR |
| | 11 | 1 | 1 | SD* | PD |
| | 12 | 8 | 2 | PR | PD |

Patients were evaluated using 3D imaging, including CT chest/abdomen/pelvis and MIBG scans as well as bilateral bone marrow aspirates and biopsies. Anti-tumor activity was defined according to INRC. NM, not measured. PD, SD, PR and CR were defined according to INRC. *Bone marrow disease cleared.

allocated to intervention (Extended Data Fig. 1). Of those excluded, seven declined to participate, five did not meet inclusion criteria, three could not obtain insurance approval and two had severe lymphopenia. Of the 14 patients allocated to intervention, two did not receive treatment; one patient's product was manufactured but not infused as the patient was receiving other treatment; and one patient's product failed manufacture likely due to severe lymphopenia at the time of collection. Median time from cell collection to infusion was 51.5 d (95% confidence interval 45–80). All patients underwent lymphodepletion with cyclophosphamide (500 mg $m^{-2}$ per dose on days −4, −3 and −2) and fludarabine (30 mg $m^{-2}$ per dose on days −4 and −3), followed by GD2-CAR.15 NKT cell infusion on day 0. Patients were infused on four DLs: $3 \times 10^6$, $1 \times 10^7$, $3 \times 10^7$ and $1 \times 10^8$ cells per $m^2$ based on GD2-CAR$^+$ NKT cell numbers. Dose escalation was guided by standard 3 + 3 design. Sixteen total infusions were given: eight patients received a single infusion, and four patients received two infusions. The infusions were well tolerated as no acute toxicities were observed on the day of cell transfer, and dose-limiting toxicities (DLTs) were not detected during the 28-d observation period after infusion. Grade 3 and 4 cytopenias of erythroid, myeloid and lymphoid lineages as well as thrombocytopenia were observed frequently and were expected after lymphodepletion (Table 2 and Supplementary Tables 1–4). Three patients experienced fevers of unknown origin, and one patient had grade 2 cytokine release syndrome (CRS), requiring a single dose of tocilizumab that rapidly stabilized the patient's blood pressure. Changes in peripheral blood cytokine levels, including increases in IL7 and IL15, indicated responses to lymphodepletion by the time of CAR-NKT infusion on day 0 (Extended Data Fig. 2a)[29]. The patient who experienced grade 2 CRS (patient 9) had the highest levels of IL1, IL6 and TNFβ of all patients evaluated at 2–3 weeks after infusion (Extended Data Fig. 2b). GD2 is expressed at low levels on peripheral nerve cells, and treatment with GD2-specific monoclonal antibodies can result in severe pain that requires aggressive management, including intravenous opioids[30–32]. On our study, none of the patients experienced such discomfort, although two patients did require opioids for localized pain due to disease progression rather than GD2-mediated peripheral nerve irritation or damage. Because many patients were heavily pre-treated with chemotherapies that impact bone marrow function before enrollment on our study, we assessed whether more than one round of lymphodepletion/CAR-NKT cell infusion was associated with increased frequency of adverse events (AEs). We did not observe any difference in the frequency and grade of AEs after the first versus after the second infusion, suggesting that multi-dosing is safe for at least two infusions in our patient population (Table 2, Supplementary Tables 1–4 and Extended Data Fig. 3). The MTD was not reached.

The secondary objective was to evaluate the anti-tumor responses of autologous GD2-CAR NKT cell infusions in patients. We employed three-dimensional (3D) imaging and bone marrow assessments using International Neuroblastoma Response Criteria (INRC)[33]. All 12 patients were evaluable after infusion, and most underwent routine disease response assessment according to the clinical protocol, except for three patients who had evidence of progressive disease (PD) on clinical examination (Table 3). After the first infusion of GD2-CAR.15 NKTs, five patients had PD, four had stable disease (SD) and three had a partial response (PR). Four patients received a second infusion and did not receive other anti-neoplastic therapies between infusions. After the second infusion, two patients (11 and 12) had PD, one patient (2) had a continued PR and one patient (10) who did not achieve remission with other post-relapse salvage therapy achieved a complete response (CR) and remained disease free for 12 months without additional anti-neoplastic therapies (Fig. 1a,b, Extended Data Fig. 4 and Supplementary Table 5).

### CAR-NKTs traffic to tumors

Manufactured products were enriched for NKT cells (median NKT purity 93.1%, range 74.1–97.2%), most of which were CD4$^+$ (median 89%, range 41.9–95.4%), and CAR expression exceeded the 20% GMP release cutoff in all cases (median 60.1%, range 20.2–87.7%)

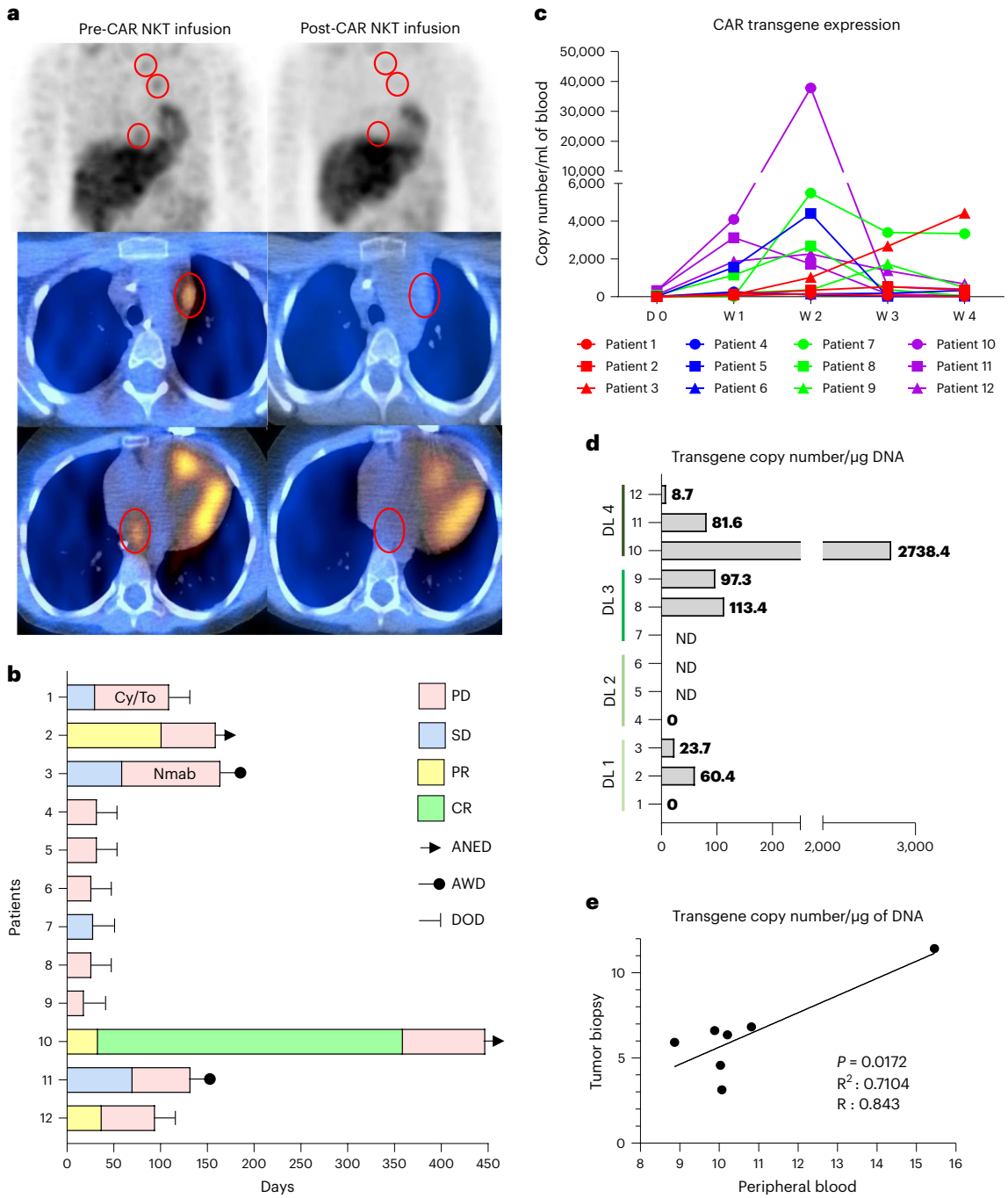


**Fig. 1 | GD2-CAR.15 NKTs expand in peripheral blood, traffic to metastatic tumor sites and induce complete remission. a**, Planar (top row) and single-photon emission CT (middle and bottom rows) images from patient 10. Red circles indicate MIBG-avid metastatic disease in thoracic cavity at baseline (left column) and resolution after two infusions of CAR-NKTs (right column). **b**, Swimmer plot representing responses to CAR-NKT infusions. Cy/To, cyclophosphamide and topotecan; Nmab, nivolumab. **c**–**e**, Peripheral blood samples were collected at indicated timepoints, and the CAR transgene was detected by qPCR. ANED, alive with no evidence of disease. AWD, alive with disease. DOD, died of disease. **c**, Transgene copy number per milliliter of peripheral blood in each patient over the course of 4 weeks after infusion. **d**, Transgene copy number per 1 µg of DNA from tumor biopsy in indicated patients at 2 weeks after infusion. **e**, Linear regression of CAR-NKT frequency in peripheral blood and tumor biopsies at 2 weeks after infusion (equation: $Y = 1.008 \times X - 4.449$). *P* value was calculated with two-tailed Pearson's correlation. D, day; W, week.

(Supplementary Fig. 1 and Supplementary Table 6). Although NKTs make up only 0.1% of human peripheral blood lymphocytes on average, and all patients received multiple cycles of myelodepleting and lymphodepleting chemotherapy before enrollment, our expansion protocol generated a median of $4.5 \times 10^8$ CAR$^+$ NKT cells per product (range $2.9–9.1 \times 10^8$), reaching the assigned DL within $10.92 \pm 2.47$ d (mean ± s.d.) of culture with repeat dosing possible for most patients.

NKTs characteristically express tissue-trafficking chemokine receptors and can effectively localize to tumors in a chemokine-dependent fashion[20,34]. This study has provided the opportunity to evaluate NKT trafficking from the peripheral blood into tumor tissues of infused patients using the CAR as a genetic marker. CAR-NKTs were detected in the peripheral blood of all patients after infusion by flow cytometry and quantitative polymerase chain reaction (qPCR), but expansion

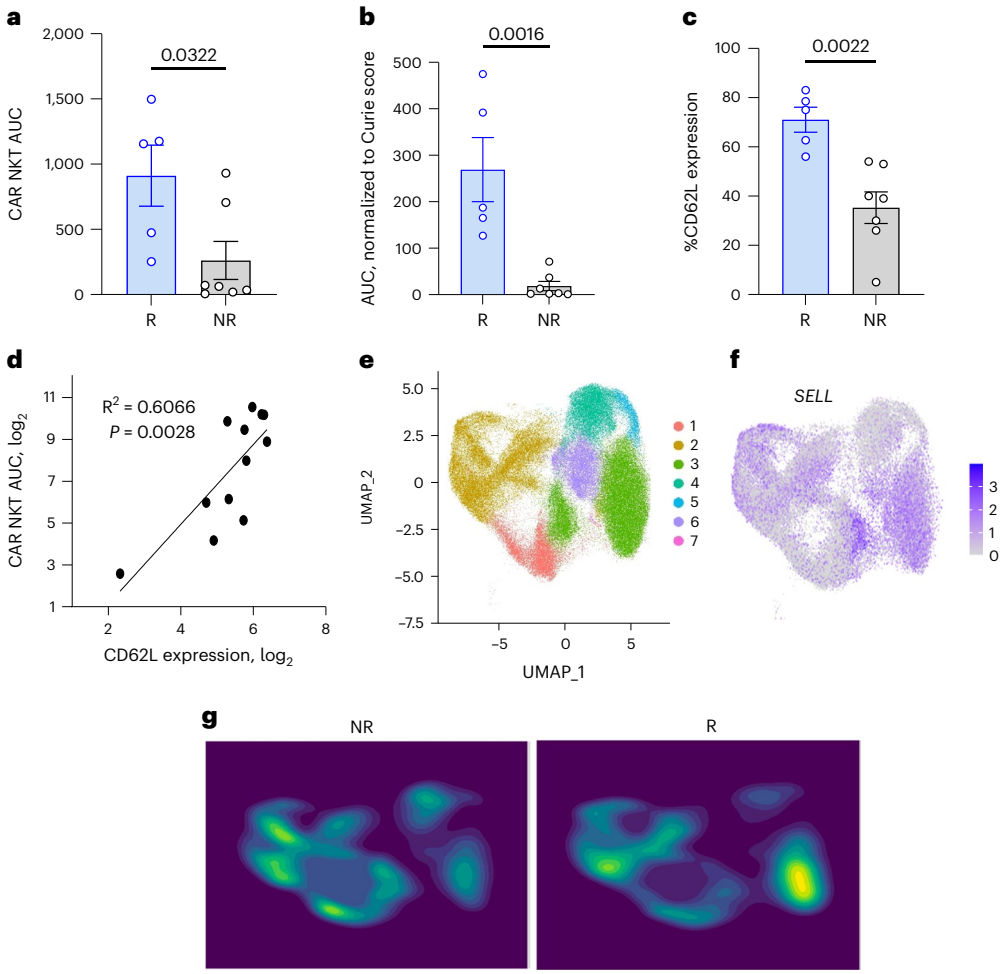


**Fig. 2 | GD2-CAR.15 NKT in vivo expansion and CD62L$^+$ expression in infusion products correlate with anti-tumor activity in patients. a**, AUC of post-infusion peripheral blood CAR-NKT numbers in responders (R, $n = 5$) versus non-responders (NR, $n = 7$). **b**, CAR-NKT AUC normalized to Curie score (quantified tumor burden) in R versus NR. **c**, CD62L$^+$ CAR-NKT frequency in pre-infusion products of R versus NR (**a**–**c** data presented as mean ± s.e.m., two-tailed paired *t*-test). **d**, Correlation analysis of CD62L expression in pre-infusion products versus CAR-NKT AUC after infusion according to linear regression model. **e**, UMAP projection showing seven unique CAR-NKT gene expression clusters in pre-infusion products identified by scRNA-seq. **f**. *SELL* (encodes CD62L) expression overlaid on UMAP projection clusters from **e**. **g**, *SELL* expression in UMAP projections corresponding to NR and R groups.

and persistence levels varied between patients and did not depend on DL (Fig. 1c and Supplementary Fig. 2). In patient 10, who achieved a CR and received no subsequent therapies, CAR-NKTs were detectable up to 18 months after infusion (Extended Data Fig. 5a). In patients who, instead, went on to receive lymphotoxic salvage regimens, CAR-NKT persistence may have been negatively impacted. To determine the impact of two infusions on CAR-NKT persistence, we compared the area under the curve (AUC) of peripheral blood CAR-NKT absolute numbers after first and second infusions in the four patients who received a second dose. Three of the four infused patients had lower CAR-NKT AUC after the second infusion, but differences between first and second infusions were not significant ($P = 0.168$; Extended Data Fig. 5b).

We also measured the presence of CAR-NKTs in tumor biopsies 2 weeks after infusion to determine whether the cells traffic to tumor sites to induce anti-tumor responses. On all four DLs, CAR-NKTs were detected in tumor tissues by qPCR, albeit at lower frequencies than in peripheral blood (Fig. 1d). Notably, we detected a significant correlation between the frequency of CAR-NKTs in the peripheral blood and tumor tissue ($R^2 = 0.71$, $R = 0.843$, $P < 0.017$; Fig. 1e), suggesting that CAR-NKTs effectively traffic to tumor sites in addition to expanding systemically.

## CAR-NKT CD62L expression associated with anti-tumor response

The presence of less differentiated immune cells in adoptive immunotherapy products can improve in vivo persistence and anti-tumor responses in preclinical tumor models[35–38]. To determine whether patients with evidence of anti-tumor activity had higher levels of CAR-NKT expansion and persistence, we compared the AUC of CAR-NKT absolute numbers in seven non-responders (patients 1, 4, 5, 6, 7, 8 and 9) versus five responders. Responders included three patients with PR or CR who met INRC (patients 2, 10 and 12) and two additional patients who did not meet objective response criteria per INRC but had evidence of anti-tumor activity based on decreased metaiodobenzylguanidine (MIBG)-avid region involvement (SD in patient 3 (30% Curie score reduction) and clearance of bone marrow involvement in patient 11 (Curie score unchanged)) (Table 3 and Supplementary Table 5). Responders had significantly higher CAR-NKT AUC than non-responders (911 versus 261.3, $P = 0.032$; Fig. 2a). Because tumor burden varied between patients at the time of enrollment, we hypothesized that higher tumor burden could be associated with decreased CAR-NKT therapeutic efficacy. To correct for differences in tumor burden, we normalized CAR-NKT AUC to the Curie score from each patient's pre-enrollment MIBG scan, a measure used to assess tumor burden in children with

NB[39]; after normalization, the difference between CAR-NKT AUC in responders versus non-responders became even more significant (269.1 versus 18.46, $P = 0.002$; Fig. 2b). Previously, our group found that the CD62L$^+$ CAR-NKT subset mediates more potent anti-tumor activity than CD62L$^-$ cells in preclinical models[38,40]. To identify potential predictors of anti-tumor response, we performed a multi-parameter immunophenotypic characterization of pre-infusion CAR-NKT cells and found a significant enrichment of CD62L$^+$ CAR-NKTs in the products of responders versus non-responders (71% versus 35.3%, $P = 0.002$; Fig. 2c and Supplementary Fig. 3). Products from responders also contained a higher frequency of CAR-NKTs expressing CD27, an additional marker of central memory-like NKTs (53% versus 34%, $P = 0.048$; Supplementary Fig. 4)[41]. We also detected a significant correlation between the frequency of CD62L$^+$ CAR-NKTs in pre-infusion products and CAR-NKT AUC in the peripheral blood after infusion ($R^2 = 0.607$, $P = 0.003$; Fig. 2d). CAR-NKTs isolated from the peripheral blood of responders and non-responders after infusion expressed similar levels of all phenotypic markers evaluated (Supplementary Fig. 5). To probe for markers of response in an unbiased manner, we performed single-cell RNA sequencing (scRNA-seq) on pre-infusion products from all patients and identified seven unique CAR-NKT cell clusters (Fig. 2e, Supplementary Fig. 6 and Supplementary Table 7). We found that most CAR-NKTs that expressed high levels of *SELL* (encodes CD62L) were concentrated in cluster 3 (Fig. 2f) and that this cluster was markedly enriched in responders versus non-responders (Fig. 2g). In addition to *SELL*, cells in cluster 3 were found to have moderately higher expression of *KLF2*, a transcription factor that drives the T lymphocyte central memory program (Supplementary Table 7)[42]. Therefore, our results indicate that the frequency of central memory-like cells in pre-infusion products may determine the ability of CAR-NKTs to expand and persist in patients with NB after infusion and ultimately mediate anti-tumor responses.

### Elevated *BTG1* expression associated with CAR-NKT exhaustion

Having established indicators of CAR-NKT clinical efficacy in pre-infusion products, we then assessed changes in CAR-NKT gene expression, phenotype and function after multiple rounds of tumor cell challenge in vitro to simulate changes that occur in vivo. To accomplish this, we performed a repeat co-culture assay in which CAR-NKT effectors are plated with fresh tumor cells every 5 d to model chronic antigen exposure (Supplementary Fig. 7a). After three cycles, the ability of CAR-NKTs to kill tumor cells and proliferate decreased, suggesting that the cells were approaching exhaustion (Extended Data Fig. 6a and Supplementary Fig. 7b). Next, we compared the post-infusion gene expression profile of CAR-NKTs isolated from patient peripheral blood versus after five cycles of in vitro repeat co-culture. We found that peripheral blood and in vitro co-cultured CAR-NKTs showed similar changes in gene expression as well as distribution of cells in four of the seven expression clusters (2, 3, 4 and 6), exemplified by the acquisition of terminal effector differentiation and loss of the naive/memory program (Extended Data Fig. 6b,c and Supplementary Fig. 7c). Compared to pre-infusion products, both post-infusion and in vitro co-cultured CAR-NKTs had numerous differentially expressed genes, including those encoding proteins involved in NK-like differentiation (*KLRC1*, *KLRC3*, *KLRC4* and *KLRD1*), cytolytic function (*GZMH*, *GMZH*, *GZMK*, *GZMM*, *LAMP1* and *NKG7*) and terminal differentiation/exhaustion (upregulation of *TBX21* and *EOMES* and downregulation of *SELL*; Extended Data Fig. 6d,e and Supplementary Fig. 7d). Notably, *BTG1* (BTG anti-proliferation factor 1) was identified as a significantly upregulated gene in both peripheral blood and in vitro tumor-challenged CAR-NKTs, and this was confirmed at the protein level (Extended Data Fig. 6d,e and Supplementary Fig. 8a). BTG1 promotes mRNA deadenylation and degradation, and it was recently described as a mediator of quiescence in murine naive T cells[43].

### BTG1 mediates hyporesponsiveness in NKT and T cells

*BTG1* expression has been reported to control the transition of murine T cells from the naive to effector state after antigenic stimulation[43]. We hypothesized that repeated stimulation of the TCR or CAR could induce upregulation of *BTG1*, resulting in mRNA loss and a hyporesponsive phenotype characteristic of both naive and exhausted T cells. To test this hypothesis, we examined BTG1 protein expression kinetics in NKTs after stimulation with CD3/CD28-specific monoclonal antibodies. We found that, although BTG1 expression was indeed downregulated in the first 4 h after TCR stimulation relative to unstimulated NKTs, after this point the trend reversed, with pronounced upregulation sustained through 7 d (Supplementary Fig. 8b,c). Similar kinetics for BTG1 expression were observed in TCR-stimulated T cells (Supplementary Fig. 9a). To determine the function of BTG1 in NKTs, we conducted gain-of-function and loss-of-function experiments by overexpressing or knocking down *BTG1*, respectively. In gain-of-function studies, NKTs transduced with a *BTG1*-overexpressing construct showed a decrease in global RNA content consistent with the known mRNA-destabilizing activity of this protein[43] (Supplementary Fig. 8d,f and Extended Data Fig. 7a). We detected 303 differentially expressed genes in NKTs overexpressing *BTG1* versus control cells (126 upregulated and 177 downregulated; Extended Data Fig. 7b). Pathway analysis revealed that NKTs overexpressing *BTG1* expressed lower levels of genes associated with the TCR, cytokine signaling and AP1 transcription factor activity than control NKTs (Extended Data Fig. 7c). Functionally, *BTG1* overexpression markedly inhibited NKT and T cell proliferation in response to TCR stimulation (Extended Data Fig. 7d and Supplementary Fig. 9b). Additionally, although expression of activation/exhaustion markers PD-1 and TIM3 was not affected (Supplementary Fig. 8g), *BTG1* overexpression did lead to an increase in activation-induced cell death and a marked decrease in NKT proliferation (Extended Data Fig. 7e,f). Together, these results suggest that BTG1 is a mediator of hyporesponsiveness in human NKT and non-naive T cells.

### Reducing *BTG1* expression enhances CAR-NKT anti-tumor activity

To explore whether *BTG1* knockdown improves the efficacy of CAR-NKT immunotherapy, we generated a set of constructs that encodes the GD2-CAR only or the GD2-CAR with IL15 (used in our clinical trial), each with and without an artificial microRNA (amiR) targeting *BTG1* (CAR.15.amiR-*BTG1*) or a scrambled microRNA control (CAR.15.amiR-SCR; Supplementary Fig. 10a). We confirmed that CAR.15.amiR-*BTG1* NKTs downregulate *BTG1* expression at both the mRNA and protein level (Supplementary Fig. 10b,c). There was not a significant difference in total fold expansion of NKTs or CAR-NKTs expressing the *BTG1* knockdown versus the scrambled control construct (Fig. 3a,b). However, *BTG1* knockdown NKTs had higher frequencies of CD62L$^+$ cells and lower frequency of PD-1$^+$ cells than NKTs expressing the scrambled control construct (Fig. 3c–e).

Next, we assessed the impact of *BTG1* knockdown on the effector function of CAR-NKTs. CAR.15.amiR-*BTG1* NKTs produced more IFN-γ than CAR.15.amiR-SCR NKTs in response to TCR stimulation (Supplementary Fig. 10d). In three independent short-term cytotoxicity assays, CAR.15.amiR-*BTG1* NKTs consistently outperformed CAR.15.amiR-SCR NKTs against GD2-high (CHLA-255) and GD2-low (CHLA-136) NB tumor cells at multiple incubation timepoints (Fig. 3f). We also compared CAR.15.amiR-*BTG1* and CAR.15.amiR-SCR NKTs in the longer five-cycle co-culture serial challenge assay; in this context, NKTs expressing the *BTG* knockdown construct mediated superior tumor control and expanded significantly more than control NKTs (Fig. 3g,h).

Finally, we compared the in vivo anti-tumor activity of *BTG1* knockdown and control CAR-NKTs using an aggressive metastatic NB xenograft mouse model that was validated during investigational new drug (IND) development for our ongoing trial (Fig. 3i). In this model, CAR.amiR-*BTG1* and CAR.15.amiR-*BTG1* NKTs mediated superior tumor

control compared to their respective scrambled controls. Moreover, CAR.15.amiR-*BTG1* NKTs mediated durable tumor regression as evidenced by the absence of bioluminescent signal from tumor cells in all 10 mice and survival of all animals in the group for more than 150 d (Fig. 3j–l). Together, these results demonstrate that *BTG1* knockdown helps protect CAR-NKTs from exhaustion and enhances their in vitro and in vivo anti-tumor activity—crucial findings for development of the next generation of NKT-based cancer immunotherapy.

## Discussion

Here we present updated interim results from our first-in-human CAR-NKT clinical trial in 12 patients with NB treated on four DLs. We show that autologous NKTs engineered to co-express a GD2-specific CAR and IL15 are well tolerated, expand numerically after infusion, localize to metastatic sites and can mediate sufficient anti-tumor activity to produce objective responses in heavily pre-treated relapsed/refractory patients with NB. We also demonstrate that the frequency of $CD62L^+$ cells and the corresponding cluster of NKTs with a central memory-like gene expression pattern correlate with the magnitude of CAR-NKT in vivo expansion and therapeutic efficacy in patients with NB. Finally, we describe an unexpected role for BTG1 as an important regulator of NKT and T cell exhaustion and find that *BTG1* downregulation enhances the anti-tumor activity of CAR-NKTs in an NB mouse model.

Thus far, we have found that patients enrolled on this study have been older than the average age of patients with high-risk NB. Patients were enrolled on a first-come/first-served basis, and we speculate that the higher average age may be due to two factors: (1) the overall worse outcome for older children with NB, leading to a higher number of older patients becoming eligible for our study, and (2) the time that elapses between diagnosis, treatment on multiple regimens and actual enrollment on the trial.

Overall, CAR-NKT cell infusions were well tolerated, with the main AEs reported being grade 3–4 hematologic events that we attribute to the cumulative effects of lymphodepleting chemotherapy and prior treatments. In a study at our center that compared cohorts treated with GD2-CAR-T cells with or without cyclophosphamide/fludarabine, grade 3–4 hematologic AEs were less common in the CAR-T-only cohort[13]. Regarding other AEs, patients on our study and most other early-phase GD2-CAR-T cell studies did not experience neuropathic pain[11,13,14], which commonly occurs with GD2-specific antibodies, including dinutuximab, and can require intravenous opioid administration[32]. Furthermore, only one patient on our study experienced grade 2 CRS, and that patient had PD; none of the five patients with evidence of anti-tumor activity developed CRS, including three with objective responses, suggesting that CAR-NKT toxicity and anti-tumor activity are not linked. In a recent GD2-CAR-T cell study, instead, two of three patients with NB with evidence of anti-tumor activity developed grade 2–3 CRS (ref. 14). Additionally, none of the responders on that study achieved an objective response despite receiving $\geq 10^8$ per $m^2$ CAR-T cells, which exceeds the dose of CAR-NKTs given at DL4 on our study. In a recent phase 1/2 trial of GD2-targeting CAR-T cells, objective responses were observed in 17 of 27 patients with NB (63%; all responders had low or undetectable disease burden), but 20 of 27 patients (74%) experienced CRS; seven patients (26%) had grade 3 liver dysfunction; and six patients (22%) suffered from grade 1–2 neuropathic pain[44]. Another phase 1 trial of CAR-T cells in patients with NB that has reported a similar objective response rate to our study used Epstein–Barr virus (EBV)-specific cytotoxic T lymphocytes and bulk T cells to express a GD2-CAR (refs. 11,12). Taken together, these observations suggest that NKTs co-expressing a GD2-CAR and IL15 may have therapeutic efficacy with similar or lower toxicity levels to conventional GD2-CAR-T cells targeting the same antigen in patients with NB. It is possible that IL15 co-expression could also enhance CAR-T therapeutic efficacy, a hypothesis that would need to be validated in future clinical trials.

Our results also provide encouraging evidence for the feasibility and safety of at least two CAR-NKT infusions. As with multiple cycles of chemotherapy, multi-dosing of cell therapeutics may be required in certain cancer types or in patients with bulky disease. Based on the reassuring safety profile and promising anti-tumor activity demonstrated in 12 patients, the study was amended to continue enrollment on two additional dose levels (DL5 = $3 \times 10^8$ and DL6 = $1 \times 10^9$ CAR-NKT cells per dose).

Consistent with our findings in preclinical models[5], CAR-NKTs localized to tumor sites in all biopsied patients on all DLs. CAR-NKT numbers in tumor tissues as quantified by qPCR correlated with expansion in the peripheral blood; this comparison was feasible in seven patients. Further characterization of CAR-NKT trafficking to NB tumors and gene expression changes in tumor-infiltrating CAR-NKTs will be crucial to inform the development of future clinical trials. CAR-NKT AUC values achieved in the peripheral blood were significantly higher in responders than non-responders, indicating that the ability of CAR-NKTs to expand after infusion determines therapeutic efficacy. Similar observations have been made with CAR-T cell products—for example, CD19-specific CAR-T cells[45]—and illustrate a distinguishing feature of cell-based therapies versus other classes of drugs.

Flow cytometry analysis of infusion products identified CD62L as a candidate biomarker of CAR-NKT expansion and anti-tumor activity after infusion. Furthermore, scRNA-seq analysis revealed that CD62L expression is concentrated in a CAR-NKT gene expression cluster that is enriched in responders versus non-responders and characterized by an expression program resembling central memory differentiation in T cells. These results are consistent with and provide clinical validation for our previous work showing that the $CD62L^+$ subset is required for human NKT in vitro expansion, in vivo persistence and durable tumor control in xenogeneic tumor models[38]. As with our findings in NKTs, $CD62L^+$ central memory T cells have been shown to possess stem-cell-like properties, with the ability to self-renew while also giving rise to effector memory and effector T cells[46]. Moreover, preservation of central memory differentiation and reduction of terminal effector differentiation in CAR-T cell products have been associated with increased in vivo persistence and therapeutic efficacy in preclinical models[2,35–38,47]. Therefore, the therapeutic potential of both T and NKT cell-based therapies could be enhanced by developing cell manufacturing protocols that favor central memory differentiation and/or inhibit effector differentiation.

**Fig. 3 | *BTG1* knockdown enhances GD2-CAR.15 NKT anti-tumor activity.** NKTs were transduced with retroviral vectors encoding the GD2-CAR with and without IL15 and amiR specific for *BTG1* or a scrambled control (Supplementary Fig. 10a). Fold expansion of total NKTs, $n = 12$ donors (**a**) and $CAR^+$ NKTs, n = 10 donors (**b**) transduced with indicated constructs (**a** and **b** data presented as mean ± s.e.m., two-tailed paired *t*-test). **c**, CD62L expression in CAR-NKTs transduced with indicated constructs, $n = 9$ donors, two-tailed paired *t*-test. **d**, CD62L expression in CAR.15.amiR-*BTG1* NKTs in $CAR^+$ versus $CAR^-$ populations, $n = 6$ donors. **e**, PD-1 expression in CAR-NKTs transduced with indicated constructs, $n = 5$ donors. **f**, Cytotoxicity of CAR.15.amiR.*BTG1* (green lines) and scrambled control NKTs (blue lines) against GD2-high CHLA255 and GD2-low CHLA136 NB cell lines assessed at indicated co-culture timepoints. *x* axis values correspond to relative effector cell numbers co-cultured at X:1 ratio with target cells, $n = 3$ technical replicates from one representative of four donors (data presented as mean ± s.d.). **g**, Residual CHLA255 tumor cell percentage in indicated groups after 5-d co-culture (E:T = 1:5), $n = 3$ donors (data presented as mean ± s.d., ordinary one-way ANOVA). **h**, Fold expansion of indicated CAR-NKT groups over the course of six co-culture cycles with CHLA255 cells, $n = 1$ representative donor of four. **i**, In vivo CAR-NKT anti-tumor activity experimental design using an aggressive metastatic NB xenograft model. **j**, Bioluminescence images of NB tumor-bearing mice injected with indicated NKT groups at specified timepoints. NT, non-transduced. **k**, Tumor burden changes based on bioluminescence images over time. **l**, Kaplan–Meier survival curves for mice in indicated groups. One experiment, 10 mice per therapeutic group, survival comparison by Gehan–Breslow–Wilcoxon test.

We used scRNA-seq to evaluate gene expression changes in pre-infusion CAR-NKT products versus (1) CAR-NKTs isolated from patient peripheral blood and (2) CAR-NKTs subject to in vitro serial co-culture with tumor cells. This allowed us to identify expression signatures that drive differentiation and hyporesponsiveness in these cells. Among the most notable significantly overexpressed genes identified was *BTG1*, a regulator of mRNA stability and recently described mediator of quiescence in naive murine T cells[43]. We found that, similarly to naive murine T cells, unstimulated human NKTs and freshly isolated naive T cells downregulate BTG1 expression shortly after TCR activation to leave the quiescent state[43]. However, continuous TCR stimulation led to re-expression and sustained upregulation of BTG1 in NKTs and T cells. Overexpression of *BTG1* in both cell types induced a finite number of differentially expressed genes but resulted in a

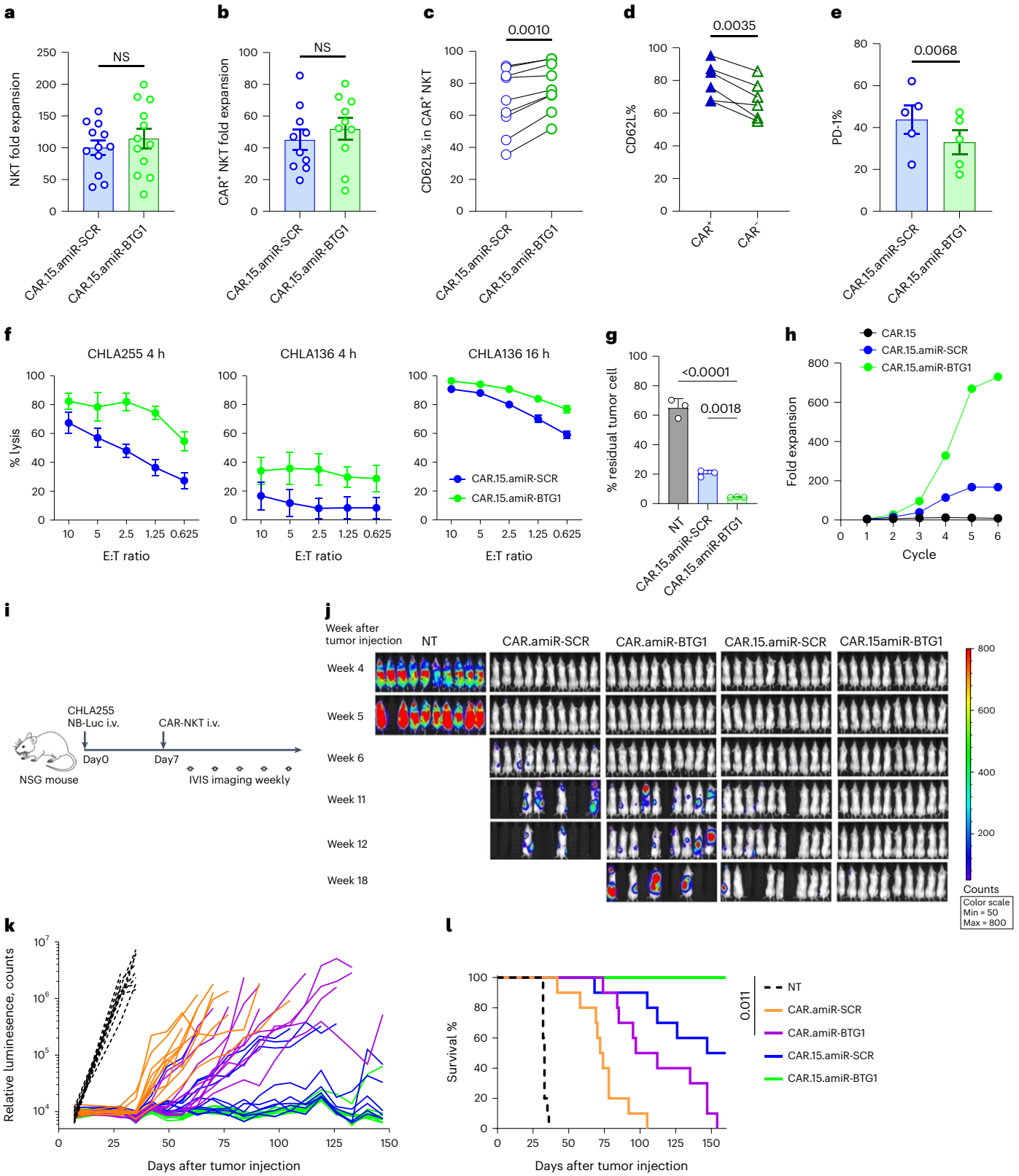

global decrease in mRNA content in the cells and lowered proliferative capacity. Of interest, the identified differentially expressed genes did not overlap with known regulators of T cell exhaustion (that is, TOX), suggesting that BTG1 uses a unique mechanism to mediate hyporesponsiveness in NKT and T cells. We speculate that, like naive T cells, exhausted T and NKT cells upregulate BTG1 to induce global mRNA degradation, contributing to the state of quiescence or hyporesponsiveness shared by naive and exhausted T cells. This hypothesis is further supported by a recent study implicating BTG1 in the progression of T cell exhaustion and the transition of exhausted T cells to a quiescent state in a murine model of chronic viral infection[48].

CAR-NKTs obtained from patient peripheral blood demonstrated a major shift in gene expression program compared to pre-infusion products, characterized by loss of proliferative potential and acquisition of an exhausted phenotype. Although the clinical significance of CAR-NKT exhaustion has not yet been established, emerging evidence from preclinical models as well as from CAR-T cell clinical studies indicates that CAR-T cell terminal differentiation and exhaustion are associated with tumor escape and disease recurrence[49–51]. Developing strategies to counteract CAR-T cell exhaustion include combining CAR-T cells with a checkpoint inhibitor[52], controlling CAR-mediated tonic signaling through genetic engineering approaches[49], modifying culture conditions with cytokines during cell manufacturing[47], inhibiting excessive CAR signaling with Src inhibitors[3] or allowing cells to rest[50]. We demonstrate that NKTs co-expressing the GD2-CAR construct used in our clinical trial with a *BTG1*-specific short hairpin RNA (shRNA) express higher levels of CD62L, lower levels of PD-1 and have increased in vitro anti-NB cytotoxicity and long-term in vivo tumor control compared to scrambled shRNA control NKTs. These results show that targeting *BTG1* expression can enhance the therapeutic potential of CAR-NKTs, informing the design of next-generation NKT-based therapeutics. Although in-depth examination of T cells and other types of immune effector cells is beyond the scope of this work, our results suggest that *BTG1* silencing may broadly benefit the development of cancer immunotherapy.

## Online content

Any methods, additional references, Nature Portfolio reporting summaries, source data, extended data, supplementary information, acknowledgements, peer review information; details of author contributions and competing interests; and statements of data and code availability are available at https://doi.org/10.1038/s41591-023-02363-y.

## References


1. Majzner, R. G. & Mackall, C. L. Clinical lessons learned from the first leg of the CAR T cell journey. *Nat. Med.* **25**, 1341–1355 (2019).
2. Batra, S. A. et al. Glypican-3-specific CAR T cells coexpressing IL15 and IL21 have superior expansion and antitumor activity against hepatocellular carcinoma. *Cancer Immunol. Res.* **8**, 309–320 (2020).
3. Mestermann, K. et al. The tyrosine kinase inhibitor dasatinib acts as a pharmacologic on/off switch for CAR T cells. *Sci. Transl. Med.* **11**, eaau5907 (2019).
4. Liu, E. et al. Use of CAR-transduced natural killer cells in CD19-positive lymphoid tumors. *N. Engl. J. Med.* **382**, 545–553 (2020).
5. Heczey, A. et al. Invariant NKT cells with chimeric antigen receptor provide a novel platform for safe and effective cancer immunotherapy. *Blood* **124**, 2824–2833 (2014).
6. Makkouk, A. et al. Off-the-shelf Vδ1 gamma delta T cells engineered with glypican-3 (GPC-3)-specific chimeric antigen receptor (CAR) and soluble IL-15 display robust antitumor efficacy against hepatocellular carcinoma. *J. Immunother. Cancer* **9**, e003441 (2021).
7. Courtney, A. N., Tian, G. & Metelitsa, L. S. Natural killer T cells and other innate-like T lymphocytes as emerging platforms for allogeneic cancer cell therapy. *Blood* **141**, 869–876 (2022).
8. Poplack, D. G. & Pizzo, P. A. *Principles and Practice of Pediatric Oncology* 6th edn (LWW, 2010).
9. Yu, A. L. et al. Long-term follow-up of a phase III study of ch14.18 (dinutuximab) + cytokine immunotherapy in children with high-risk neuroblastoma: COG study ANBL0032. *Clin. Cancer Res.* **27**, 2179–2189 (2021).
10. Dotti, G., Gottschalk, S., Savoldo, B. & Brenner, M. K. Design and development of therapies using chimeric antigen receptor-expressing T cells. *Immunol. Rev.* **257**, 107–126 (2014).
11. Pule, M. A. et al. Virus-specific T cells engineered to coexpress tumor-specific receptors: persistence and antitumor activity in individuals with neuroblastoma. *Nat. Med.* **14**, 1264–1270 (2008).
12. Louis, C. U. et al. Antitumor activity and long-term fate of chimeric antigen receptor-positive T cells in patients with neuroblastoma. *Blood* **118**, 6050–6056 (2011).
13. Heczey, A. et al. CAR T cells administered in combination with lymphodepletion and PD-1 inhibition to patients with neuroblastoma. *Mol. Ther.* **25**, 2214–2224 (2017).
14. Straathof, K. et al. Antitumor activity without on-target off-tumor toxicity of GD2-chimeric antigen receptor T cells in patients with neuroblastoma. *Sci. Transl. Med.* **12**, eabd6169 (2020).
15. Kronenberg, M. & Gapin, L. The unconventional lifestyle of NKT cells. *Nat. Rev. Immunol.* **2**, 557–568 (2002).
16. Metelitsa, L. S. et al. Human NKT cells mediate antitumor cytotoxicity directly by recognizing target cell CD1d with bound ligand or indirectly by producing IL-2 to activate NK cells. *J. Immunol.* **167**, 3114–3122 (2001).
17. Song, L. et al. Vα24-invariant NKT cells mediate antitumor activity via killing of tumor-associated macrophages. *J. Clin. Invest* **119**, 1524–1536 (2009).
18. Cortesi, F. et al. Bimodal CD40/Fas-dependent crosstalk between iNKT cells and tumor-associated macrophages impairs prostate cancer progression. *Cell Rep.* **22**, 3006–3020 (2018).
19. Godfrey, D. I., MacDonald, H. R., Kronenberg, M., Smyth, M. J. & Van Kaer, L. NKT cells: what's in a name? *Nat. Rev. Immunol.* **4**, 231–237 (2004).
20. Metelitsa, L. S. et al. Natural killer T cells infiltrate neuroblastomas expressing the chemokine CCL2. *J. Exp. Med.* **199**, 1213–1221 (2004).
21. Tachibana, T. et al. Increased intratumor Vα24-positive natural killer T cells: a prognostic factor for primary colorectal carcinomas. *Clin. Cancer Res.* **11**, 7322–7327 (2005).
22. Molling, J. W. et al. Low levels of circulating invariant natural killer T cells predict poor clinical outcome in patients with head and neck squamous cell carcinoma. *J. Clin. Oncol.* **25**, 862–868 (2007).
23. Motohashi, S., Okamoto, Y., Yoshino, I. & Nakayama, T. Anti-tumor immune responses induced by iNKT cell-based immunotherapy for lung cancer and head and neck cancer. *Clin. Immunol.* **140**, 167–176 (2011).
24. Exley, M. A. et al. Adoptive transfer of invariant NKT cells as immunotherapy for advanced melanoma: a phase I clinical trial. *Clin. Cancer Res.* **23**, 3510–3519 (2017).
25. Motohashi, S. et al. A phase I-II study of α-galactosylceramide-pulsed IL-2/GM-CSF-cultured peripheral blood mononuclear cells in patients with advanced and recurrent non-small cell lung cancer. *J. Immunol.* **182**, 2492–2501 (2009).
26. Yamasaki, K. et al. Induction of NKT cell-specific immune responses in cancer tissues after NKT cell-targeted adoptive immunotherapy. *Clin. Immunol.* **138**, 255–265 (2011).
27. Exley, M. A. et al. Adoptive transfer of invariant NKT cells as immunotherapy for advanced melanoma: a phase 1 clinical trial. *Clin. Cancer Res.* **23**, 3510–3519 (2017).

28. Heczey, A. et al. Anti-GD2 CAR-NKT cells in patients with relapsed or refractory neuroblastoma: an interim analysis. *Nat. Med.* **26**, 1686–1690 (2020).
29. Dudley, M. E. et al. Adoptive cell therapy for patients with metastatic melanoma: evaluation of intensive myeloablative chemoradiation preparative regimens. *J. Clin. Oncol.* **26**, 5233–5239 (2008).
30. Mody, R. et al. Irinotecan-temozolomide with temsirolimus or dinutuximab in children with refractory or relapsed neuroblastoma (COG ANBL1221): an open-label, randomised, phase 2 trial. *Lancet Oncol.* **18**, 946–957 (2017).
31. Yu, A. L. et al. Phase I trial of a human-mouse chimeric anti-disialoganglioside monoclonal antibody ch14.18 in patients with refractory neuroblastoma and osteosarcoma. *J. Clin. Oncol.* **16**, 2169–2180 (1998).
32. Yu, A. L. et al. Anti-GD2 antibody with GM-CSF, interleukin-2, and isotretinoin for neuroblastoma. *N. Engl. J. Med.* **363**, 1324–1334 (2010).
33. Park, J. R. et al. Revisions to the International Neuroblastoma Response Criteria: a consensus statement from the National Cancer Institute Clinical Trials Planning Meeting. *J. Clin. Oncol.* **35**, 2580–2587 (2017).
34. Liu, D. et al. IL-15 protects NKT cells from inhibition by tumor-associated macrophages and enhances antimetastatic activity. *J. Clin. Invest.* **122**, 2221–2233 (2012).
35. Klebanoff, C. A. et al. Central memory self/tumor-reactive $CD8^+$ T cells confer superior antitumor immunity compared with effector memory T cells. *Proc. Natl Acad. Sci. USA* **102**, 9571–9576 (2005).
36. Graef, P. et al. Serial transfer of single-cell-derived immunocompetence reveals stemness of $CD8^+$ central memory T cells. *Immunity* **41**, 116–126 (2014).
37. Gattinoni, L. et al. Acquisition of full effector function in vitro paradoxically impairs the in vivo antitumor efficacy of adoptively transferred $CD8^+$ T cells. *J. Clin. Invest.* **115**, 1616–1626 (2005).
38. Tian, G. et al. $CD62L^+$ NKT cells have prolonged persistence and antitumor activity in vivo. *J. Clin. Invest.* **126**, 2341–2355 (2016).
39. Decarolis, B. et al. Iodine-123 metaiodobenzylguanidine scintigraphy scoring allows prediction of outcome in patients with stage 4 neuroblastoma: results of the Cologne Interscore Comparison Study. *J. Clin. Oncol.* **31**, 944–951 (2013).
40. Ngai, H. et al. IL-21 selectively protects $CD62L^+$ NKT cells and enhances their effector functions for adoptive immunotherapy. *J. Immunol.* **201**, 2141–2153 (2018).
41. Ngai, H. et al. LEF1 drives a central memory program and supports antitumor activity of natural killer T cells. *Cancer Immunol. Res.* **11**, 171–183 (2023).
42. Schober, S. L. et al. Expression of the transcription factor lung Krüppel-like factor is regulated by cytokines and correlates with survival of memory T cells in vitro and in vivo. *J. Immunol.* **163**, 3662–3667 (1999).
43. Hwang, S. S. et al. mRNA destabilization by BTG1 and BTG2 maintains T cell quiescence. *Science* **367**, 1255–1260 (2020).
44. Del Bufalo, F. et al. GD2-CART01 for relapsed or refractory high-risk neuroblastoma. *N. Engl. J. Med.* **388**, 1284–1295 (2023).
45. Maude, S. L. et al. Tisagenlecleucel in children and young adults with B-cell lymphoblastic leukemia. *N. Engl. J. Med.* **378**, 439–448 (2018).
46. Gattinoni, L. et al. A human memory T cell subset with stem cell-like properties. *Nat. Med.* **17**, 1290–1297 (2011).
47. Xu, Y. et al. Closely related T-memory stem cells correlate with in vivo expansion of CAR.CD19-T cells and are preserved by IL-7 and IL-15. *Blood* **123**, 3750–3759 (2014).
48. Giles, J. R. et al. Shared and distinct biological circuits in effector, memory and exhausted $CD8^+$ T cells revealed by temporal single-cell transcriptomics and epigenetics. *Nat. Immunol.* **23**, 1600–1613 (2022).
49. Long, A. H. et al. 4-1BB costimulation ameliorates T cell exhaustion induced by tonic signaling of chimeric antigen receptors. *Nat. Med.* **21**, 581–590 (2015).
50. Weber, E. W. et al. Transient rest restores functionality in exhausted CAR-T cells through epigenetic remodeling. *Science* **372**, eaba1786 (2021).
51. Good, C. R. et al. An NK-like CAR T cell transition in CAR T cell dysfunction. *Cell* **184**, 6081–6100(2021).
52. John, L. B. et al. Anti-PD-1 antibody therapy potently enhances the eradication of established tumors by gene-modified T cells. *Clin. Cancer Res.* **19**, 5636–5646 (2013).

[1]Department of Pediatrics, Center for Advanced Innate Cell Therapy, Baylor College of Medicine, Houston, TX, USA. [2]Department of Medicine, Center for Cell and Gene Therapy, Baylor College of Medicine, Houston, TX, USA. [3]Department of Radiology, Texas Children's Hospital, Baylor College of Medicine, Houston, TX, USA. [4]Biostatistics and Data Management Resource, Dan L. Duncan Comprehensive Cancer Center, Baylor College of Medicine, Houston, TX, USA. [5]Department of Pediatrics, Cincinnati Children's Hospital, Cincinnati, OH, USA. [6]Immunai, Inc., New York, NY, USA. [7]Lineberger Comprehensive Cancer Center, University of North Carolina at Chapel Hill, Chapel Hill, NC, USA. ✉e-mail: heczey@bcm.edu; lsmeteli@txch.org

## Methods

### Study development and design

The phase 1 clinical trial 'GD2 Specific CAR and Interleukin-15 Expressing Autologous NKT Cells to Treat Children with Neuroblastoma' (GINAKIT2; NCT03294954) was reviewed and approved by the Protocol Review Committee, the Institutional Biosafety Committee and the Institutional Review Board at Baylor College of Medicine (BCM; H-41033) as well as the Recombinant DNA Advisory Board of the National Institutes of Health and the US Food and Drug Administration (FDA) (IND number 17815). The study was conducted in accordance with Declaration of Helsinki principles. All participants and/or their legal guardians provided written informed consent/assent upon enrollment and before administration of the cells. The GINAKIT2 study is a phase 1 clinical trial using standard 3 + 3 dose escalation as described in the clinical protocol (Supplementary Appendix). Based on standard 3 + 3 design and no DLTs observed on DLs 1–4, the maximum number of patients is 24 and may be fewer depending on safety parameters determined on DLs 5 and 6. Patients were enrolled between 20 August 2018 and 17 December 2021. Self-reported sex was collected and is listed in enrollment and outcome tables of the manuscript. Sex/gender are not independent factors for outcomes in patients with high-risk NB, and, given the sample size of 12, sex/gender-based analyses were not performed in this study.

### Study eligibility

**Treatment inclusion criteria.** Inclusion criteria included: relapsed or refractory high-risk neuroblastoma; life expectancy of at least 12 weeks; age greater than 1 year and less than 21 years; Karnofsky/Lansky score of 60% or greater; absolute neutrophil count ≥500 per microliter; platelet count ≥20,000 per microliter (patients may be transfused to obtain a platelet count >20,000 per microliter); pulse oxygen ≥90% on room air; aspartate aminotransferase less than three times the upper limit of normal; total bilirubin and creatinine less than 1.5 times the upper limit of normal; must have recovered from the acute toxic effects of all prior chemotherapy based on the enrolling physician's assessment (if some effects of chemotherapy are expected to last long term, patient is eligible if meeting other eligibility criteria); absence of human anti-mouse antibodies (HAMAs) before enrollment for patients who have received prior therapy with murine antibodies; must have autologous transduced NKTs with ≥20% expression of GD2-specific CAR; informed consent and assent (as applicable) obtained from parent/guardian and child; and weight more than 12 kg.

**Treatment exclusion criteria.** Exclusion criteria included: rapidly progressive disease; currently receiving any investigational drugs; history or hypersensitivity to murine protein-containing products; and cardiomegaly or bilateral pulmonary infiltrates on chest radiograph or computed tomography (CT). However, patients with cardiomegaly on imaging may be enrolled if they have an assessment of cardiac function (that is, echocardiogram (ECHO) or multigated acquisition (MUGA)) within 3 weeks of starting protocol therapy that is within normal limits. Additionally, patients with bilateral pulmonary infiltrates on imaging may be enrolled if the lesions are not consistent with active NB (that is, negative on functional imaging with positron emission tomography (PET) or MIBG or by pathologic assessment). Other exclusion criteria included tumor potentially causing airway obstruction; pregnancy or lactation or not willing to use birth control; currently receiving immunosuppressive drugs, such as corticosteroids, tacrolimus or cyclosporine; severe previous toxicity from cyclophosphamide or fludarabine based on the enrolling physician's assessment; or HIV infection.

### Clinical safety and outcome assessment

AEs were collected from the start of lymphodepletion until 28 d after infusion and described according to the Common Terminology Criteria for Adverse Events version 4. A DLT was defined as (1) any hematological or non-hematological grade 3–5 toxicity considered to be primarily related to CAR-NKT cells; (2) CRS and neurological toxicities grades 3 and 4—expected reactions associated with CAR-based immunotherapy (for example, fever and hypotension) lasting less than 72 h were not considered DLTs, whereas symptoms lasting more than 72 h were considered DLTs; and (3) any other unexpected grade 3 or higher toxicity thought to be related to or resulting from CRS or due to neurological toxicity. Grades 3 and 4 CRS or neurological toxicities that persisted beyond 72 h were reported to the FDA in an expedited fashion and considered DLTs. Anti-tumor responses were defined by comparing standard 3D imaging (CT and magnetic resonance imaging), MIBG scans and bone marrow aspirates/biopsies from pre- and post-CAR-NKT infusion. Anti-tumor responses were examined using the INRC (ref. 33) and by measuring differences in pre-infusion and post-infusion Curie scoring[39]. For correlative studies, 'responders' were classified as those meeting response criteria according to the INRC or who had SD per INRC but had additional evidence of anti-tumor activity, including patient 3 who had reduction of Curie score not reaching the 50% cutoff for PR and patient 11 with clearance of bone marrow disease and unchanged Curie score. An independent Data Safety Monitoring Committee monitored the safety of the study.

### Clinical-grade vector production

The clinical-grade vector encoding the GD2-CAR.15 construct was produced in the current GMP (cGMP) facility of the Center for Cell and Gene Therapy at BCM. In brief, the SFG plasmid encoding the GD2-CAR.15 construct was transfected into HEK293T cells, which produce Gibbon ape leukemia virus-pseudotyped, Moloney murine leukemia virus-derived gamma-retroviral particles. The clinical vector was validated, tested according to cGMP guidance, cryopreserved and stored at −80 °C until use.

### CAR-NKT cell manufacturing

Peripheral blood mononuclear cells (PBMCs) were isolated from peripheral blood leukapheresis products using Ficoll gradient purification, and NKTs were isolated using a special lot of anti-iNKT microbeads (Miltenyi Biotec, tested according to FDA guidelines by BioReliance) and the CliniMACS instrument (Miltenyi Biotec). Enriched NKTs were then stimulated with α-galactosylceramide (Glycosyn, cGMP grade)-pulsed PBMCs and cultured with IL2 and IL21 (NCI, 200 U $ml^{-1}$ and CellGenix, 10 ng $ml^{-1}$, respectively). Cells were transduced with retroviral particles encoding the GD2-CAR.15 construct in RetroNectin-coated plates (Takara Bio) for 72 h and then washed, replated and cultured at 38 °C for 9–15 d. CAR-NKT products that did not expand sufficiently by day 10 (patients 1, 2, 6 and 7) were restimulated with α-galactosylceramide-pulsed PBMCs and further expanded until sufficient numbers were met for the assigned DL. At the end of manufacture, products were evaluated by trypan blue staining and flow cytometry, and GD2-CAR transgene copy number was determined by qPCR.

### Transgene copy number assessment

GD2-CAR transgene copy number was evaluated in peripheral blood and tumor biopsy samples. Genomic DNA was extracted using the QIAamp DNA Blood Minikit (Qiagen) according to the manufacturer's instructions, and transgene copy number was measured by the TaqMan qPCR gene expression assay using primers (forward: 5′-GCTGCACCAACTGTATCCATCTT-3′; reverse: 5′-GGTCCAGACTGCT GAAGCT-3′) and probe (5′-CACCCGACCCACCACC-3′) sequences complementary to the GD2-CAR sequence (Applied Biosystems). qPCR was performed in 25-µl reaction volumes using the ABI 7900HT Sequence Detection System (Applied Biosystems). Copy number was normalized to 1 µg of DNA isolated from PBMCs. Transgene copy number was calculated per milliliter of peripheral blood to avoid the artificial increase in copy number that may arise due to lower overall white blood cell numbers after cyclophosphamide/fludarabine chemotherapy.

### Flow cytometry analyses

GD2-CAR-NKTs were detected in peripheral blood and patient biopsy samples using the following antibodies: FITC-conjugated anti-TCR Vβ11 (clone C21, Beckman Coulter, 1:12.5 dilution); PE-conjugated anti-iNKT (6B11, BD Biosciences, 1:10 dilution); BV421-conjugated anti-CD3 (SK7, BD Biosciences, 1:10 dilution); and an anti-idiotype GD2-CAR antibody (1A7, 1:400 dilution) produced in-house using murine hybridoma HB-11786 (American Type Culture Collection) and custom conjugated with APC (BioLegend). Evaluation of patient products also included PE-Cy7-conjugated anti-CD62L (DREG56, 1:20 dilution) and APC-H7-conjugated anti-CD4 (SK3, 1:10 dilution), both from BD Biosciences. The following antibodies were used for in-depth phenotypic analysis of patient PBMCs: BUV563-conjugated anti-CCR4 (1G1, 1:100 dilution); BUV395-conjugated anti-CD4 (L200, 1:100 dilution); BV421-conjugated anti-CD62L (DREG-56, 1:200 dilution); BV650-conjugated anti-CD366 (7D3, 1:100 dilution); BB700-conjugated anti-CD27 (L128, 1:100 dilution); BV510-conjugated anti-CD197 (2-L1-A, 1:100 dilution); FITC-conjugated anti-CD3 (UCHT1, 1:10 dilution), all from BD Biosciences; BUV737-conjugated anti-CD223 (3DS223H, 1:100 dilution) and PE-conjugated anti-CD279 (J105, 1:100 dilution), both from Thermo Fisher Scientific; and BV785-conjugated anti-CD39 (A1, 1:100 dilution) and PE-Cy7-conjugated anti-iNKT (6B11, 1:100 dilution), both from BioLegend. The following antibodies were used for flow cytometry studies relating to BTG1: BV421 mouse anti-human CD45RA (HI100, 1:50 dilution); PE-Cy7 mouse anti-human CD3 (UCHT1, 1:50 dilution); and BV421 anti-human-iNKT (6B11, 1:50 dilution), all from BD Biosciences; and PE anti-human CD279 (PD-1) (EH12.2H7, 1:50 dilution); BV421 anti-human CD366 (Tim-3) (F38-2E2, 1:50 dilution) and FITC anti-human CD62L (DREG-56, 1:50 dilution), all from BioLegend. All flow samples were run using an LSRII five-laser flow cytometer or a Symphony A5 five-laser flow cytometer (BD Biosciences, Texas Children's Hospital Cancer Center Flow Cytometry Core) or a Symphony A1 four-laser flow cytometer (BD Biosciences) and analyzed using BD FACSDiva software version 6.0 and FlowJo version 10.6.1 software (TreeStar).

### *BTG1* overexpression experiments

The human BTG1 amino acid sequence was obtained from UniProt (P62324), reverse transcribed to the nucleotide sequence and codon optimized for expression in humans. The cDNA encoding BTG1 was cloned into a GFP plasmid by HiFi DNA assembly (New England Biolabs) to generate a GFP-P2A-BTG1 plasmid.

**Amino acid sequence.** MHPFYTRAATMIGEIAAAVSFISKFLRTK-GLTSERQLQTFSQSLQELLAEHYKHHWFPEKPCKGSGYRCIRINHKM-DPLIGQAAQRIGLSSQELFRLLPSELTLWVDPYEVSYRIGEDGSICVLYEAS-PAGGSTQNSTNVQMVDSRISCKEELLLGRTSPSKNYNMMTVSG.

**Nucleotide sequence.** ATGCATCCCTTCTACACCCGGGCCGCCACCAT-GATAGGCGAGATCGCCGCCGCCGTGTCCTTCATCTCCAAGTTTCTC-CGCACCAAGGGGCTCACGAGCGAGCGACAGCTGCAGACCTTCAGC-CAGAGCCTGCAGGAGCTGCTGGCAGAACATTATAAACATCACTG-GTTCCCAGAAAAGCCATGCAAGGGATCGGGTTACCGTTGTATTCG-CATCAACCATAAAATGGATCCTCTGATTGGACAGGCAGCACAGCG-GATTGGACTGAGCAGTCAGGAGCTGTTCAGGCTTCTCCCAAGTGAACT-CACACTCTGGGTTGACCCCTATGAAGTGTCCTACAGAATTGGAGA-GGATGGCTCCATCTGTGTGCTGTATGAAGCCTCACCAGCAGGAGGTAG-CACTCAAAACAGCACCAACGTGCAAATGGTAGACAGCCGAATCAGCTG-TAAGGAGGAACTTCTCTTGGGCAGAACGAGCCCTTCCAAAAACTA-CAATATGATGACTGTATCAGGTTAA.

### *BTG1* knockdown and vector generation

Vectors were based on the SFG retroviral backbone used in the clinical trial. Expression cassettes encoding the GD2-CAR, IL15 and *BTG1*-specific or scrambled shRNA sequences were generated by overlapping PCR. The DSIR tool (http://biodev.cea.fr/DSIR/) was used to select the *BTG1*-targeting shRNA sequence, which was then cloned into the non-targeting miR-155 backbone to generate amiRs. Cassettes encoding the GD2-CAR with or without IL15 and the *BTG1*-targeting amiR or scrambled amiR were constructed by inserting the appropriate amiR sequence 3′ into the GD2-CD28-CD3ζ-IL15 backbone.

*BTG1*-targeting sequence (DSIR6): TACAACGGTAACCCGATCCCT.

Non-targeting sequence (Scramble): AAATGTACTGCGCGTGG AGAC.

### RNA isolation

RNA was isolated using the RNeasy Mini Kit (Qiagen) according to the manufacturer's instructions. RNA was quantified by measuring absorbance at 260/280 nm using a NanoDrop One device, and integrity was verified by analysis on a TapeStation system (Agilent Technologies). Samples passed quality control when the 260/80 ratio was ≥1.8 and RNA integrity was ≥6.8.

### Gene expression analysis using RNA-seq

Bulk RNA-seq was conducted by Novogene using the Illumina NovaSeq PE150 platform, a paired-end sequencing technology with 150-bp read length. Raw reads were first cleared of adaptor sequences. Sequencing quality was assessed using FastQC software (version 0.11.2). Quality metrics, such as sequence quality scores, sequence duplication and adaptor content, were considered to determine whether to apply filtering criteria before genome mapping. Clean reads were mapped against the human reference genome (GRCh38.p13 assembly) using read aligner HISAT2 (version 2.1.0). Mapped reads were subsequently assembled into transcripts or genes using StringTie software (version 1.3.5). Differential gene expression analysis was performed on raw counts using the R statistical package DESeq2 (version 1.28.1). Genes with a more than two-fold increase (fold change (FC) ≥ 2) and $P < 0.05$ were considered significantly upregulated, and genes with a more than two-fold decrease (FC ≤ 0.5) and $P < 0.05$ were considered significantly downregulated. Non-coding genes were filtered out of the analyses.

### Cell culture

Human NB cell lines CHLA-136 and CHLA-255 were established and maintained as previously described[53]. Cell lines were maintained in IMDM supplemented with 20% heat-inactivated FBS (Gibco, Invitrogen) and 2 mM GlutaMAX (Gibco, Invitrogen) without antibiotics.

### qPCR

qPCR for *BTG1* expression was performed on a CFX96 Touch Real-Time PCR Detection System (Bio-Rad) using pre-designed SYBR Green-compatible primers (Sigma-Aldrich) and the iTaq Universal SYBR Green One-Step Kit according to the manufacturer's instructions. All signals were quantified using the ΔCT method and normalized to 18S rRNA expression.

BTG1_FW: CTTCATCTCCAAGTTTCTCC.

BTG1_RV: CAGAGGATCCATTTTATGGTTG.

18S RNAr FW: CTCAACACGGGAAACCTCAC.

18S RNAr RV: CGCTCCACCAACTAAGAACG.

### Western blot analysis

Cells were dissociated with RIPA buffer (Sigma-Aldrich) and protease inhibitors (Thermo Fisher Scientific). Protein concentrations were determined using a Bio-Rad protein assay with BSA as standard. Samples were denatured in Laemmli buffer (Bio-Rad) containing 5% 2-mercaptoethanol (Bio-Rad) at 95 °C for 6 min. Cell lysate (50 µg per lane) was run on a 12% SDS polyacrylamide gel (Bio-Rad) and transferred to PVDF membrane (Immobilon-P, Millipore). Membranes were blocked with milk powder in Tris-buffered saline (TBS) (Sigma-Aldrich) + 0.1% Tween 20 (Sigma-Aldrich) and then probed with primary antibodies followed by horseradish peroxidase-conjugated secondary antibodies.

Blots were developed using SuperSignal West Dura Extended Duration Substrate (Thermo Fisher Scientific) and exposed to GeneMate Blue Basic Autoradiography Film (BioExpress). Protein levels were normalized to loading controls. Primary antibodies included recombinant anti-BTG1 antibody (EPR8274) (Abcam), actin (AC-15)(Sigma-Aldrich) and tubulin (10D8) (Santa Cruz Biotechnology). Secondary antibodies included goat anti-rabbit (31460) (Bio-Rad) and goat anti-mouse (31430) (Bio-Rad). For western blotting, all primary antibodies were diluted 1:1,000, and all secondary antibodies were diluted 1:5,000.

### Multiplex cytokine assay

Serum cytokine levels were measured using the Milliplex MAP magnetic bead-based human cytokine pre-mixed 38-plex kit (EMD Millipore) on the Luminex 200 system with xPONENT software (Luminex) according to the manufacturer's instructions.

### Cytotoxicity assays

Short-term cytotoxicity of parental and GD2-CAR NKTs against CHLA-255 or CHLA-136 was evaluated using 4-h and 16-h luciferase assays as previously described[54]. In addition, $GFP^+$ CHLA-255 cells were seeded in six-well plates at $2 \times 10^6$ cells per well overnight, and NT or CAR-NKT cells were added at a 1:5 effector-to-target (E:T) ratio. On day five of co-culture, cells were collected, and target and effector cell frequencies were measured by flow cytometry based on CD3 and GFP expression, respectively.

### Serial tumor challenge assay

Patient CAR-NKT cells and CHLA-255 NB cells transduced with GFP were co-cultured in a 24-well plate using fresh culture medium at a 1:1 ratio, respectively. Every other day, 50 U $ml^{-1}$ human IL2 was added. Five days later, cells were harvested, quantified by trypan blue exclusion and analyzed for NKT and NB cell markers by flow cytometry. CAR-NKT cells were then replated 1:1 with fresh NB cells in fresh cell culture medium to start the next round of tumor co-culture. This process was repeated for five (patient-derived) and six (healthy donor-derived) rounds.

### Proliferation and apoptosis assays

NKTs were labeled using the CellTrace Violet Cell Proliferation Kit (C34557, Invitrogen) and stimulated in plates coated with anti-CD3/CD28 antibody (OKT3/CD28.2, BD Biosciences). Cell proliferation was evaluated on day 5 by flow cytometry measuring CellTrace Violet (C34557, Thermo Fisher Scientific) dilution. In addition, early stages of apoptosis were measured on day 3 by staining with PE-Annexin V (BD Biosciences) and Fixable Viability Dye eFluor 780 (65-0865-14, eBioscience), followed by flow cytometry.

### PMA/Ionomycin assay

CAR-NKT cells were stimulated with anti-CD3/CD28 beads (11452D, Gibco), and exhaustion phenotype was confirmed by flow cytometry. CAR-NKT cells were stimulated with PMA/ionomycin and GolgiStop (BD Biosciences) for 3 h. Intracellular staining for IFN-γ (clone B27, 562988, BD Biosciences) was performed after fixation and permeabilization.

### In vivo experiments evaluating GD2-CAR NKTs with *BTG1* knockdown

NSG mice were obtained from The Jackson Laboratory and maintained at the BCM animal care facility. For in vivo therapeutic experiments, mice were injected intravenously with $1 \times 10^6$ firefly luciferase-labeled CHLA255 cells. On day seven, mice were treated intravenously with $3 \times 10^6$ CAR-NKTs, followed by intraperitoneal injection of IL2 (2,000 U per mouse) every other day for 2 weeks. Tumor growth was assessed weekly by bioluminescent imaging. Animal experiments were performed according to Institutional Animal Care and Use Committee (IACUC)-approved protocol AN-5194 at BCM.

### scRNA-seq data processing

scRNA-seq reads were aligned to the human transcriptome (GRCh38), and unique molecular identifier (UMI) counts were quantified to generate a gene–barcode matrix using the Cell Ranger pipeline (10x Genomics, version cellranger-5.0.1). Cellular indexing of transcriptomes and epitopes by sequencing (CITE-seq) antibody expression matrices were generated using the Cell Ranger pipeline (10x Genomics, version cellranger-5.0.1). The reference genome version GRCh38 was modified to include the GD2-CAR sequence and exclude all endogenous immunoglobulin sequences with homologous sequences to the GD2-CAR. TCR reads were aligned to the modified GRCh38 reference genome (10x Genomics, version cellranger-5.0.1). Cells were demultiplexed and assigned to their respective samples using proprietary Immunai algorithms. Cells were then filtered based on the number of UMIs, detected total number of genes and more specifically housekeeping genes as well as levels of mitochondrial gene expression to remove empty droplets, low-quality cells, dying cells and doublets. Cutoffs for these metrics were chosen by the more conservative values between hard predefined cutoffs and calculated cutoffs per sample that were based on the interquartile range. For cluster analysis of all immune cells, expression counts of both genes and surface proteins were normalized and scaled. To integrate all samples from the same project into a joint data structure, batch effects were mitigated using an integration algorithm that preserves biological diversity while removing artifacts (Harmony[55]). Harmony was applied to gene expression data and protein expression data separately. For RNA-seq, the full expression matrix was first reduced to an Immunai-curated marker gene list containing more than 2,000 genes associated with cellular identities across all PBMC types and then submitted to principal component analysis. The first 20 principal components were next submitted to Harmony batch correction. For CITE-seq, because of its lower dimensionality, the full expression matrix was submitted to Harmony batch correction. The batch-corrected RNA-seq and CITE-seq data fed into a multimodal nearest neighbor calculation (weighted nearest neighbors[56]), which formed the basis for clustering using graph community clustering methods and two-dimensional embedding using uniform manifold approximation and projection (UMAP). Only CAR-NKT cells with positive counts of the GD2-CAR construct, TRAV10, and TRBV25-1 were kept for further analysis. Gene expression markers for each cluster were computed using the FindAllMarkers function in Seurat version 4.0.6, comparing non-parametric variables related to cells from one cluster to all other cells in the dataset using the Wilcoxon rank-sum test. For differential gene expression analysis, differentially expressed genes were discovered using Limma-Voom version 3.46.0 from EdgeR package version 3.32.1. First, the mean expression of each sample was computed across all single cells, and then we fitted a linear regression model where responder status, or the timepoint, was the independent variable and looked for genes that had significantly different expression levels between different conditions. We tested the following conditions in CAR-NKT cells: responder versus non-responder, pre-infusion versus in vitro stimulation, in vitro stimulation versus post-infusion and pre-infusion versus post-infusion.

### Statistical analysis

A Student's *t*-test was used for two groups; one-way ANOVA with post hoc Tukey correction was used for continuous variables among more than two groups; and two-way ANOVA was used when two independent variables were considered. Correlations between two continuous variables were assessed with Pearson correlation and simple linear regression models. Survival estimates were assessed by the Kaplan–Meier method and compared using the Gehan–Breslow–Wilcoxon test. Statistics were computed using GraphPad Prism 9.0 (GraphPad Software). Differences were considered significant when the *P* value was less than 0.05.

### Reporting summary

Further information on research design is available in the Nature Portfolio Reporting Summary linked to this article.

## Data availability

All requests for raw and analyzed data and materials should be directed to L.S.M. and will be promptly reviewed by the Baylor College of Medicine Licensing Group to verify if the request is subject to any intellectual property or confidentiality obligations. Patient-related data not included in the paper were generated as part of the clinical trial and may be subject to patient confidentiality. Any data and materials that can be shared will be released via a material transfer agreement. All raw data for single-cell sequencing are deposited in the Gene Expression Omnibus under accession number GSE223071. Source data are provided with this paper.

## References


53. Keshelava, N. et al. Histone deacetylase 1 gene expression and sensitization of multidrug-resistant neuroblastoma cell lines to cytotoxic agents by depsipeptide. *J. Natl Cancer Inst.* **99**, 1107–1119 (2007).
54. Xu, X. et al. NKT cells coexpressing a GD2-specific chimeric antigen receptor and IL15 show enhanced in vivo persistence and antitumor activity against neuroblastoma. *Clin. Cancer Res.* **25**, 7126–7138 (2019).
55. Korsunsky, I. et al. Fast, sensitive and accurate integration of single-cell data with Harmony. *Nat. Methods* **16**, 1289–1296 (2019).
56. Hao, Y. et al. Integrated analysis of multimodal single-cell data. *Cell* **184**, 3573–3587 (2021).


## Acknowledgements


The authors are grateful to M. Brenner, H. Heslop and personnel of the cGMP facility at the Center for Cell and Gene Therapy for manufacturing CAR-NKTs, including A. Jacques, J. Sritabal-Ramirez, H. Hu, K. Matzar and R. Al Hussien. We also thank K. Kukreja of the Interventional Radiology section and P. Srivaths, director of the Pheresis Service, of Texas Children's Hospital, as well as staff of the Flow Cytometry Core Laboratory of the Texas Children's Cancer and Hematology Center and the Single Cell Genomics Core at Baylor College of Medicine, for excellent technical assistance. This work was supported by grants or contracts from Alex's Lemonade Stand Foundation for Childhood Cancer, St. Baldrick's Foundation, the American Cancer Society (to L.S.M. and A.H.) and Athenex, Inc. We thank the Cancer Prevention and Research Institute of Texas (CPRIT) for support under grant no. RP180785.


## Author contributions

A.H. and L.S.M. designed the clinical trial. A.H. wrote the clinical protocol and was the principal investigator of the clinical trial. G.D., L.S.M., A.H., X.X. and G.T. developed the CAR construct selected for the trial and tested it in NKT cells. A.H., A.C.S. and B.D.W. performed pre-therapy and post-therapy patient clinical evaluation. H.Z. and B.M. generated CAR-NKT cell products in the cGMP facility. A.N.C., C.M.A., N.G., S.G.T. and P.R. processed clinical samples and performed flow cytometry, qPCR and Luminex. X.X. performed serial tumor challenge assay. A.M., M.S., C.X., C.S. and D.K.W. performed and analyzed scRNA-seq. C.Z. analyzed bulk RNA-seq. X.X., G.A.B., M.S.W., T.D. and Y.L. tested in vitro BTG1 function in NKT and T cells. X.X. and L.G. performed therapeutic experiments in mice. B.G. and T.W. provided regulatory and statistical support for the clinical trial. The manuscript was written by A.H. and L.S.M. and edited by E.J.D.P. All authors discussed and interpreted results.

## Competing interests

A.H., A.N.C., G.T., X.X, G.D. and L.S.M. are co-inventors on pending patent applications that relate to the use of NKTs in cancer immunotherapy, including those that have been licensed by Baylor College of Medicine to Athenex, Inc. for commercial development. Athenex, Inc. provided research support for this project (to L.S.M.) via a sponsored research agreement with Baylor College of Medicine. G.A.B., L.G., C.M.A., N.G., P.R., M.S.W., Y.L., C.Z., T.D., E.J.D.P., A.C.S., H.Z., B.M., S.G.T., B.G., T.W., B.D.W., A.M., M.S., C.X., C.S. and D.K.W. declare no competing financial interests.

## Additional information

**Extended data** is available for this paper at https://doi.org/10.1038/s41591-023-02363-y.

**Supplementary information** The online version contains supplementary material available at https://doi.org/10.1038/s41591-023-02363-y.


**Correspondence and requests for materials** should be addressed to Andras Heczey or Leonid S. Metelitsa.



**Peer review information** *Nature Medicine* thanks Joseph Fraietta, Beibei Guo and the other, anonymous, reviewer(s) for their contribution to the peer review of this work. Primary handling editor: Saheli Sadanand, in collaboration with the *Nature Medicine* team.



**Reprints and permissions information** is available at www.nature.com/reprints.

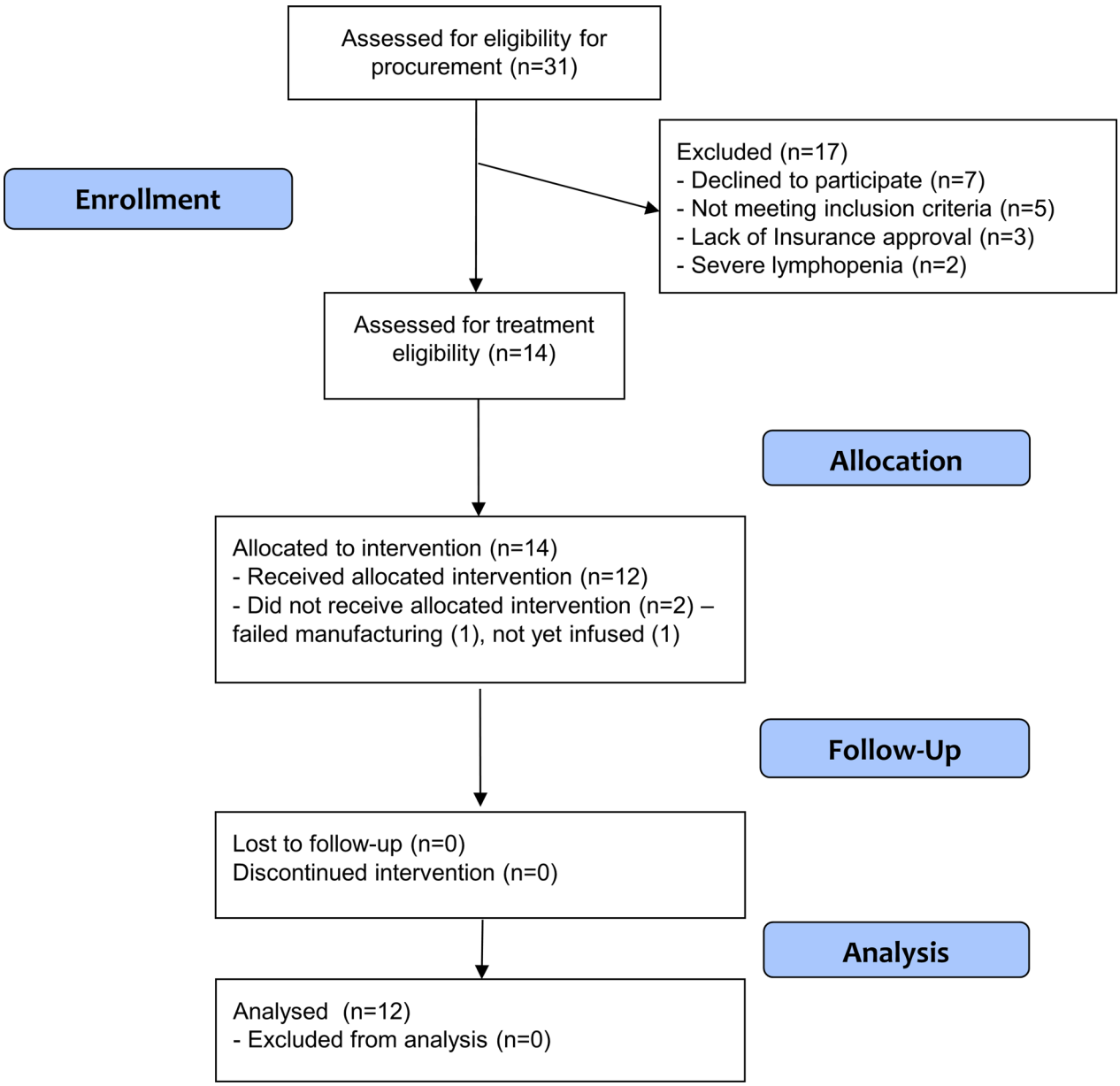


**Extended Data Fig. 1 | Consort flow diagram summarizing enrollment on the GINAKIT2 study.** Enrollment is conducted in two phases: procurement (manufacturing of the cell product) and treatment (infusion of the cell product). The study is a single arm, Phase 1 clinical trial and patients were enrolled on a first come/first served basis. Received allocated intervention on DL1: 3, DL2: 3, DL3: 3 and DL4 4 patients.

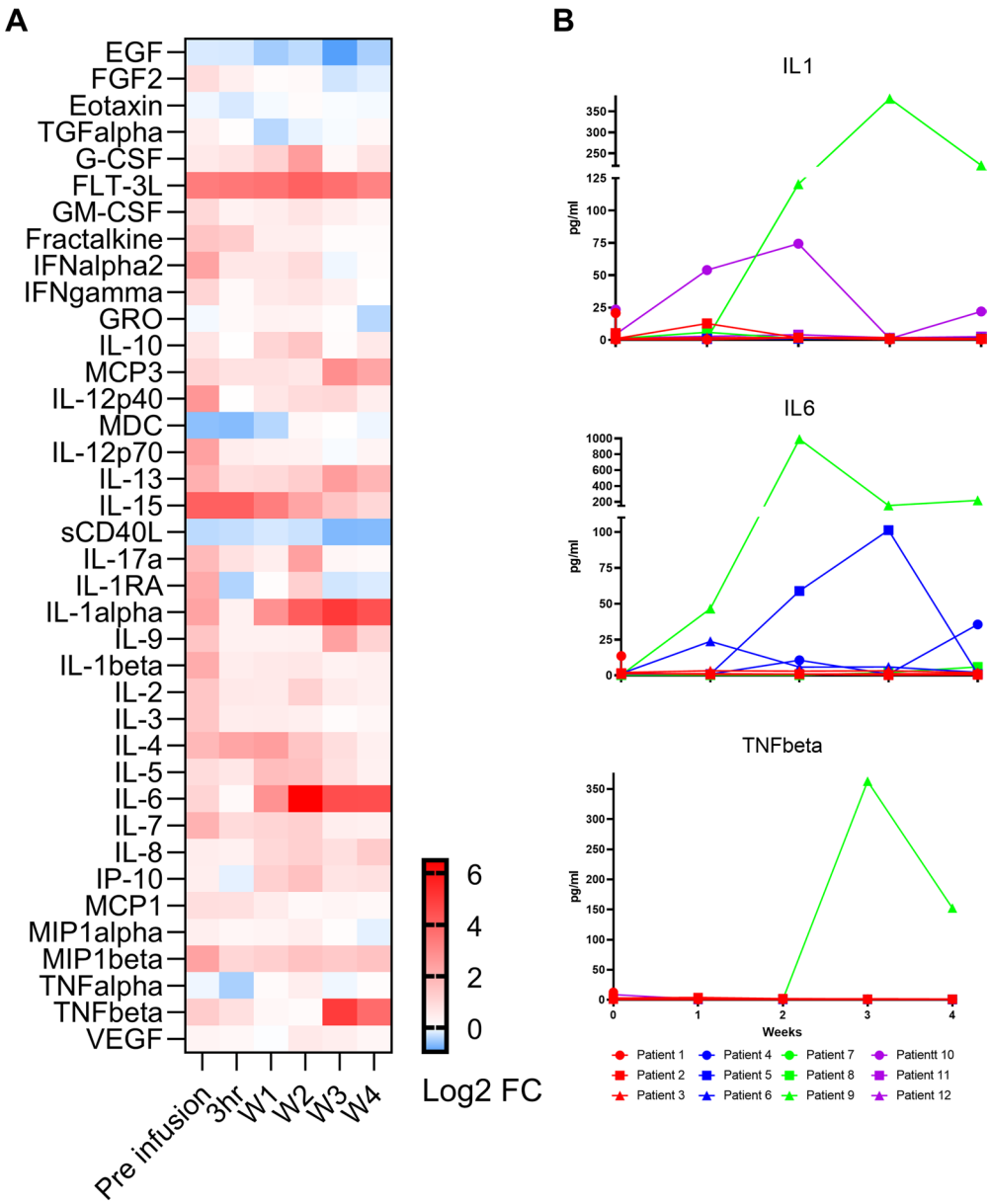


**Extended Data Fig. 2 | Serum cytokine and chemokine levels in patients infused with GD2-CAR.15 NKTs.** A. Mean fold change (FC) compared to baseline (day −4) of 38 evaluated cytokines and chemokines in patient peripheral blood samples collected at indicated timepoints quantified by Luminex. B. Absolute values (pg/mL) of IL1, IL6 and TNFbeta over four weeks in all patients.

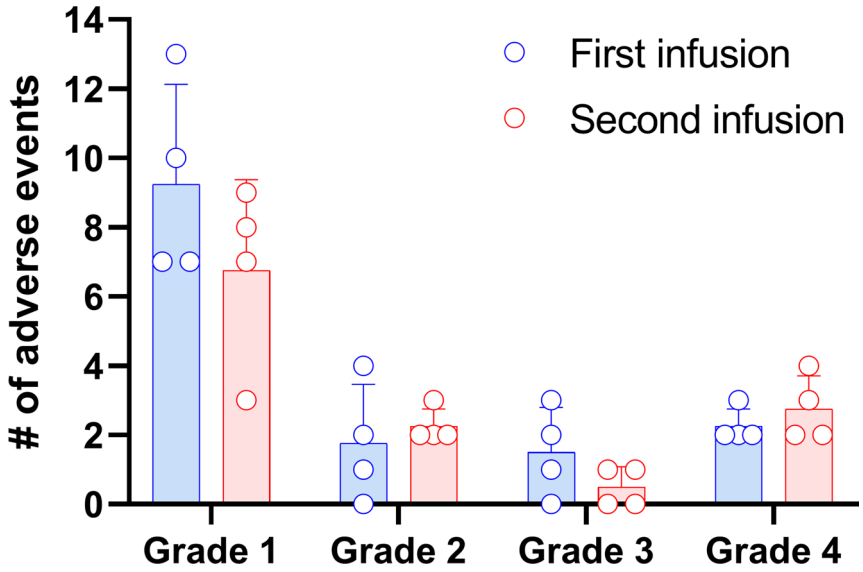


**Extended Data Fig. 3 | Frequency and severity of adverse events following first and second GD2-CAR.15 NKT infusions.** Toxicity parameters were assessed and graded according to the Common Terminology Criteria for Adverse Events version 4 from the start of lymphodepletion (day −4) until four weeks after each infusion (day 28). n = 4 patients. Data presented as mean +/− SD.

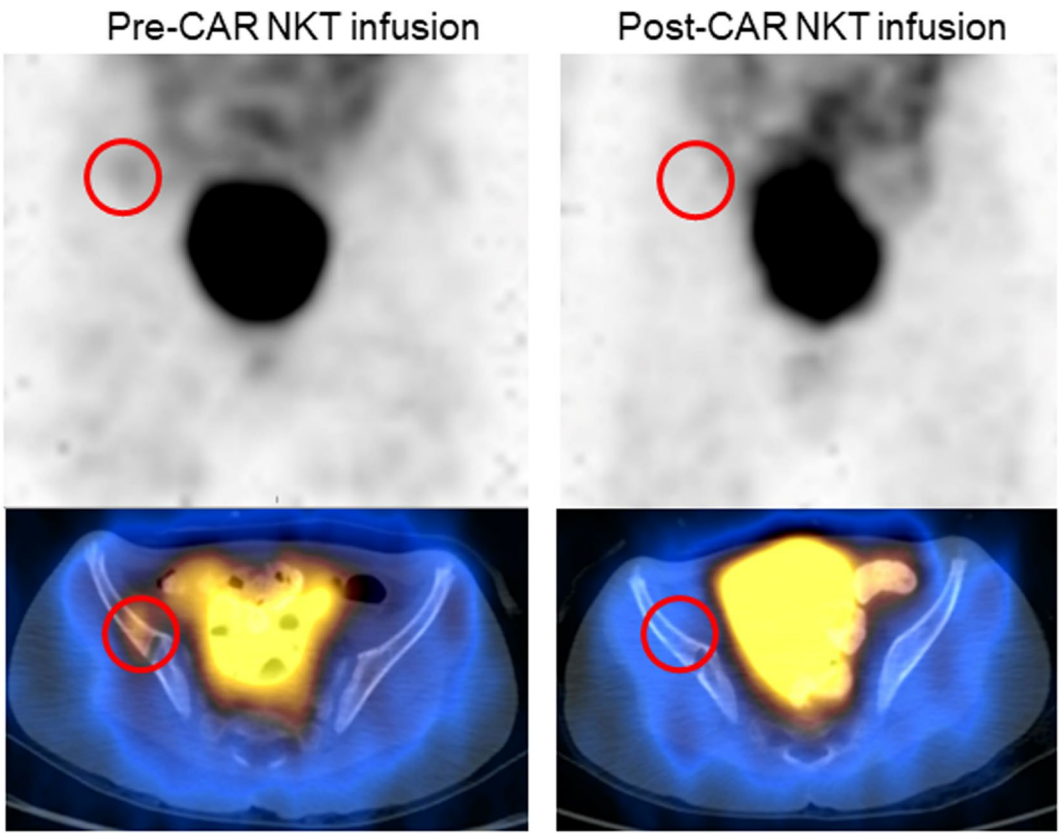


**Extended Data Fig. 4 | Antitumor response in patient 12.** Pre- and post-GD2-CAR NKT infusion images from MIBG scans. Planar images (top row) and fused SPECT-CT images (bottom row) show pelvic bone metastasis (red circle) visible prior to infusion (left column) and complete resolution after infusion (right column). Note: MIBG-avid regions in the middle of the image correspond to bladder with urine containing MIBG.

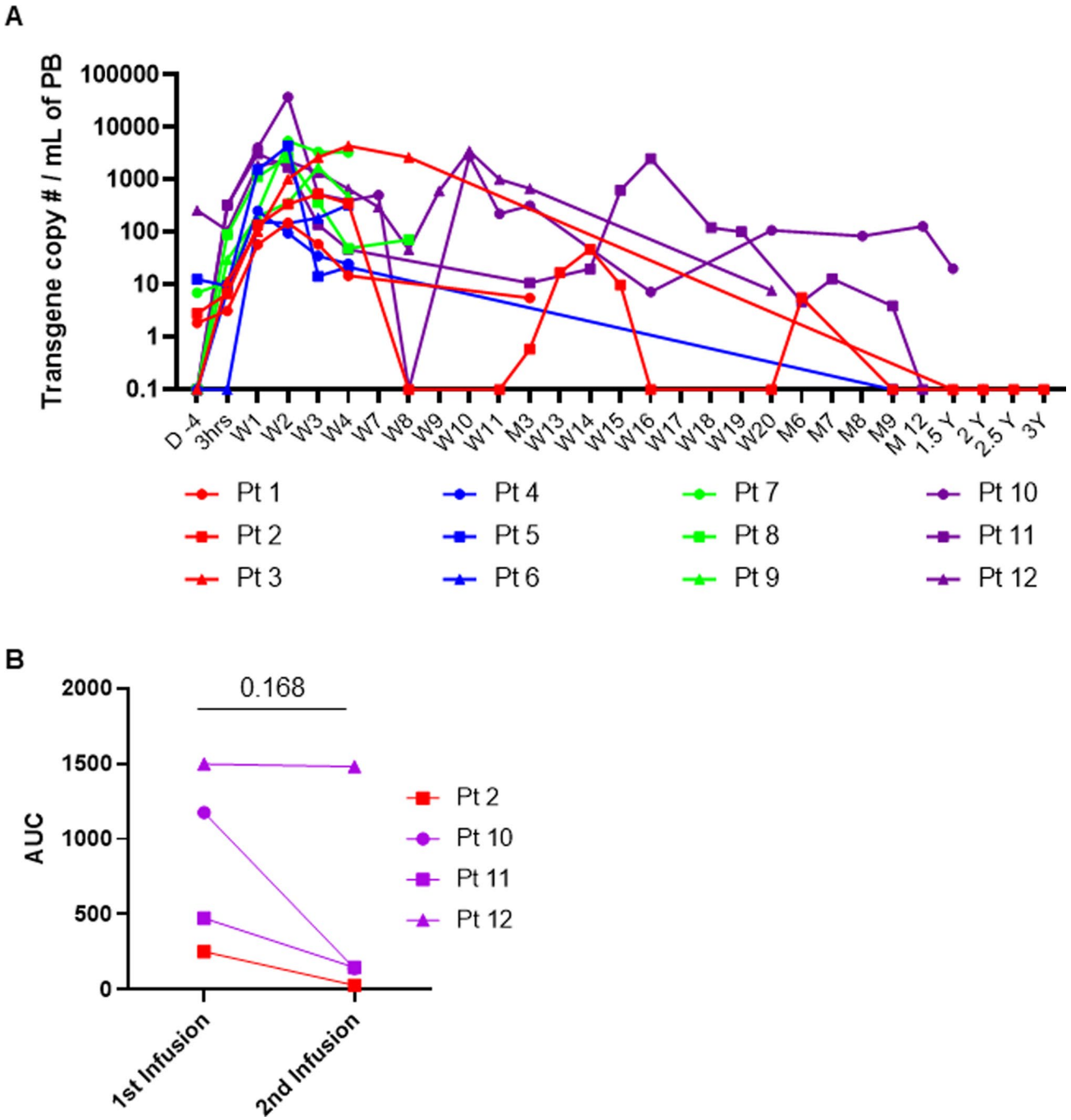


**Extended Data Fig. 5 | Long-term expansion and persistence of GD2-CAR.15 NKTs in patients with relapsed or refractory neuroblastoma.** A. Peripheral blood (PB) samples were collected at indicated timepoints and the CAR transgene was detected by quantitative PCR. Patients 10 and 12 were reinfused at approximately week 8 (W8); patients 2 and 11 were reinfused at approximately three months (M3). B. AUC of peripheral blood CAR-NKT absolute numbers in four patients receiving repeat infusions. Two-tailed paired T test.

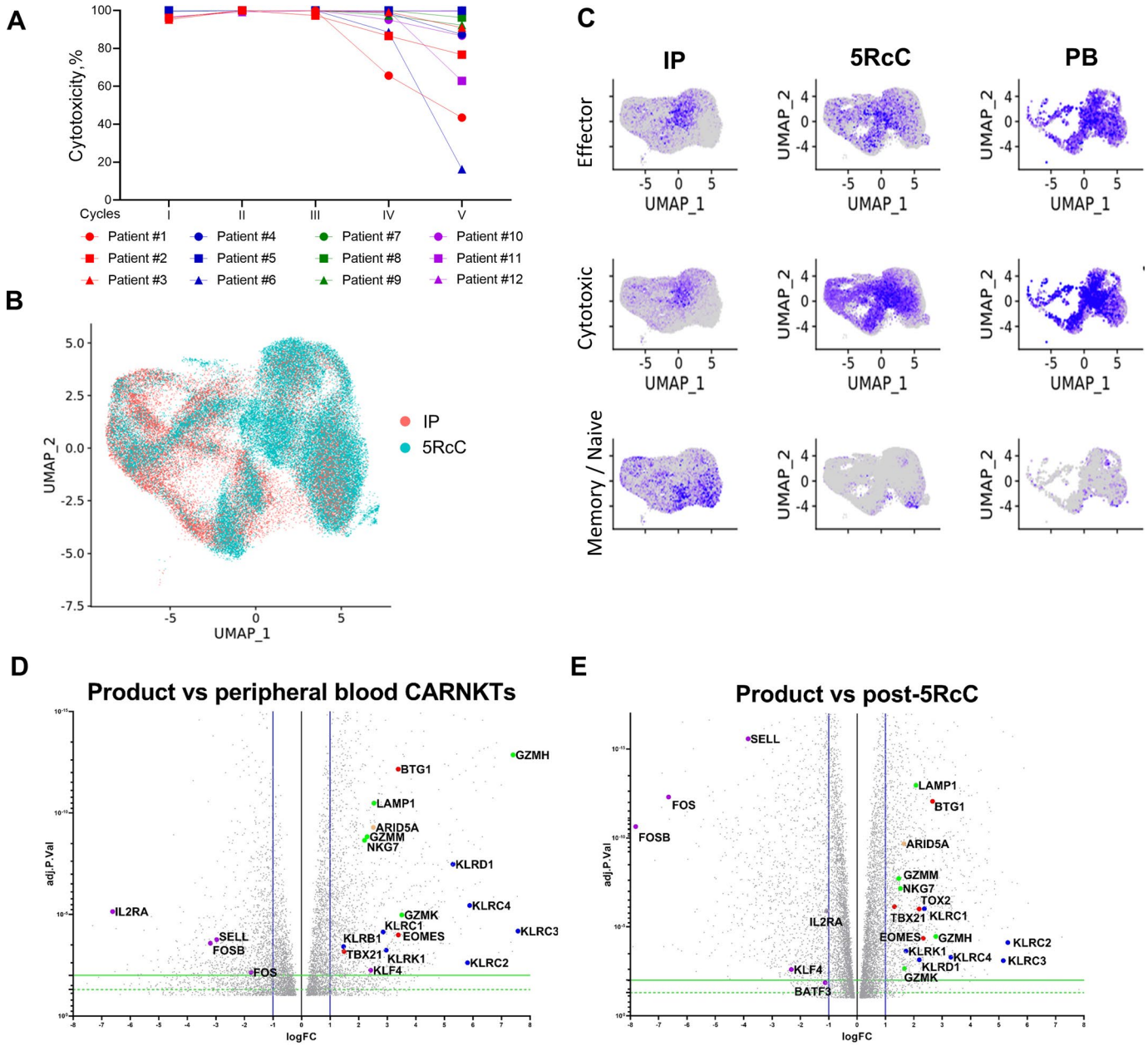


**Extended Data Fig. 6 | *BTG1* expression is elevated in exhausted CAR-NKTs.** A. Cytotoxicity of CAR-NKTs from patient pre-infusion products against CHLA255 NB cells over the course of five repeat co-culture cycles. B. UMAP projections of gene expression profiles measured by scRNAseq from pre-infusion products (IP) and CAR-NKTs following five-cycle repeat co-culture with tumor cells (5RcC). C. UMAP projection of gene expression in CAR-NKTs from pre-infusion products (IP), post-5RcC (5RcC), and isolated from peripheral blood (PB) post-infusion. D, E. Volcano plots showing differentially expressed genes in pre-infusion products versus peripheral blood CAR-NKTs (D) and versus post-5RcC CAR-NKTs (E).

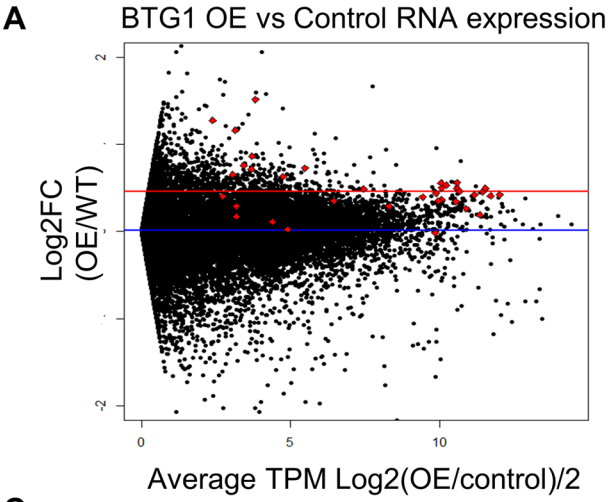


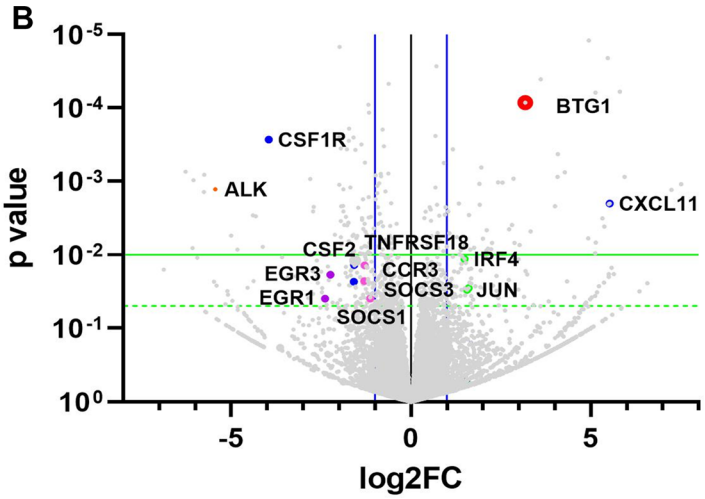


C

| Pathways | P-value | Adjp-value | Genes |
|---|---|---|---|
| TNF-alpha Signaling via NF-kB | 7.24E-06 | 2.32E-04 | FOSL1;SOCS3;EGR1;DUSP2;EGR3;CSF1;DUSP1;FOS;CD69;SGK1 |
| IL-6/JAK/STAT3 Signaling | 8.95E-05 | 0.001431 | CCR1;SOCS3;SOCS1;CSF1;EBI3;CD9 |
| IL-2/STAT5 Signaling | 2.74E-04 | 0.002924 | MYO1E;ECM1;SOCS1;CSF1;TNFRSF18;SPRY4;TNFSF11;TNFRSF4 |
| Calcineurin-regulated NFAT-dependent transcription in lymphocytes | 3.97E-05 | 0.004251 | IL4;FOSL1;EGR1;EGR3;FOS |
| Downstream signaling in naive CD8+ T cells | 2.26E-04 | 0.007466 | FOSL1;EGR1;TNFRSF18;FOS;TNFRSF4 |
| ErbB1 downstream signaling | 2.52E-04 | 0.007466 | RPS6KA3;EGR1;DUSP1;SRC;FOS;DUSP6 |
| AP-1 transcription factor network | 2.79E-04 | 0.007466 | IL4;FOSL1;EGR1;DUSP1;FOS |
| Allograft Rejection | 0.00676 | 0.054084 | CCR1;IL4;SOCS1;CSF1;CD47;EIF4G3 |
| Androgen Response | 0.009885 | 0.063267 | RPS6KA3;ACTN1;SGK1;FADS1 |
| Estrogen Response Late | 0.026448 | 0.10579 | DUSP2;EGR3;CD9;FOS;SGK1 |
| Interferon Gamma Response | 0.026448 | 0.10579 | HELZ2;SOCS3;SOCS1;CD69;CMKLR1 |
| Inflammatory Response | 0.026448 | 0.10579 | CSF1;SLC31A2;EBI3;CD69;CMKLR1 |
| Interferon Alpha Response | 0.047712 | 0.169643 | HELZ2;CSF1;CD47 |

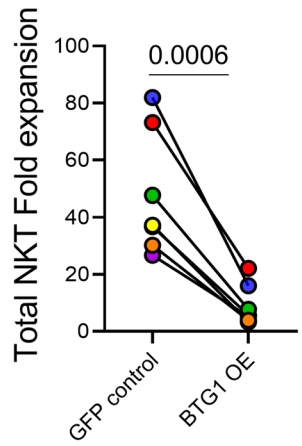


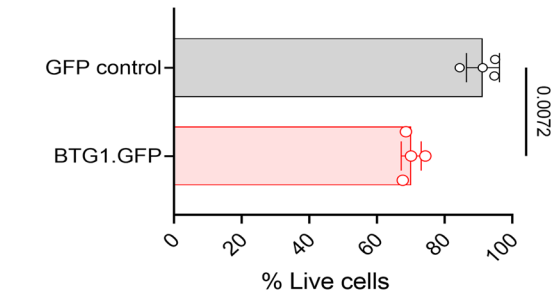


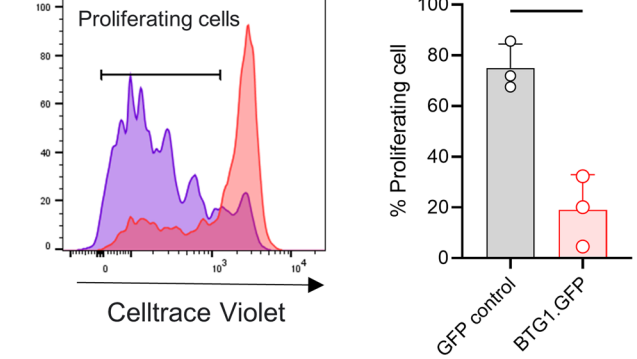


**Extended Data Fig. 7 | Overexpression (OE) of BTG1 reduces global RNA expression and proliferative capacity in NKTs.** A. Total RNAseq reads from BTG1-OE and control NKTs. Red and blue lines indicate fold change from nuclear or mitochondrial transcripts, respectively. B. Volcano plot showing differentially expressed genes in BTG1-OE NKTs versus control NKTs. Blue vertical lines correspond to two-fold change on log2 scale; green dashed and solid lines represent $p < 0.05$ and $<0.01$, respectively. C. Pathway enrichment analysis showing gene expression programs enriched in BTG1-OE NKTs. Fisher's exact test was used to calculate the probability of observing overlap between the input gene set and the pathway or gene set database by chance. P-values were adjusted for multiple testing using the Benjamini-Hochberg method to control for false discovery rate. D. Fold expansion of BTG1-OE vs control NKTs, n = 6 donors, two-tailed paired T test. E, F. Survival of NKTs stimulated with anti-CD3/CD28 monoclonal antibodies and evaluated with annexin V and fixable viability dye e780 on day 3, n = 4 (E) and CellTrace Violet dilution measured on day 5, n = 3 (F), (E-F data presented as mean +/− SD: two-tailed paired T test).